GENETIC CONTROL OF GUMMY STEM BLIGHT RESISTANCE AND RIND THICKNESS IN WATERMELON

by

LINCOLN ADAMS

(Under the Direction of Cecilia McGregor)

ABSTRACT

This study examined two traits related to economic losses in watermelon, resistance to gummy stem blight (GSB) and rind thickness (RTH). QTLseq was used to identify QTL for resistance to GSB isolate 12178A (*Stagonosporopsis citrulli*) in a population derived from PI 189225. QTLseq identified 4 QTL contributing resistance to *S. citrulli,* and the QTL on chromosome 5 (*Qgsb5.2*) was confirmed as a novel QTL. Three watermelon populations were used to investigate the association of fruit size QTL (*QFD2.2* and *QFSI3.1*) with RTH and the rind thickness to fruit diameter ratio (RRP) and to confirm *QRTH5.1*. Our results indicated that the association of fruit size QTL with RTH and RRP were dependent on their interaction with *QRT5.1* and the genetic background of the population. KASP marker assays developed in this study for *Qgsb5.2, QFD2.2* and *QRTH5.1* should allow breeders to select QTL for resistance to *S. citrulli,* and for fruit diameter, and rind thickness.

INDEX WORDS: Watermelon, *Citrullus lanatus*, *Citrullus amarus,* Gummy Stem Blight, *Stagonosporopsis citrulli*, Resistance, Rind Thickness, Fruit Diameter, Rind Ratio Percentage, QTLseq, QTL Mapping

GENETIC CONTROL OF GUMMY STEM BLIGHT RESISTANCE AND RIND THICKNESS IN WATERMELON

by

LINCOLN ADAMS

B.S., The University of Georgia, 2018

A Thesis Submitted to the Graduate Faculty of The University of Georgia in Partial Fulfillment of the Requirements for the Degree

MASTER OF SCIENCE

ATHENS, GEORGIA

2021

GENETIC CONTROL OF GUMMY STEM BLIGHT RESISTANCE AND RIND THICKNESS IN WATERMELON

by

LINCOLN ADAMS

Major Professor:	Cecilia McGregor
Committee:	Marin Brewer
	Zenglu Li

Electronic Version Approved:

Ron Walcott
Vice Provost for Graduate Education and Dean of the Graduate School
The University of Georgia
December 2021

DEDICATION

For my mother, Hope Adams, and my grandfather, De Wood, who always pushed me to achieve my dreams and believed in me, even when I did not believe in myself.

ACKNOWLEDGEMENTS

I would like to thank the following people, either for their invaluable assistance with the research contained within, or for the support and inspiration that lead me here:

My entire family, for their endless emotional and financial support in the face of my repeated failures.

Dr. Cecilia McGregor, for her invaluable mentorship, guidance, and support, as well as years of funding and the use of her laboratory and field facilities.

Dr. Marin Brewer and Dr. Zenglu Li, for their contributions as members of my graduate committee.

Dr. Winnie Gimode, for sharing her wealth of knowledge and experience on GSB research.

Dr. Reeve Legendre and Samuel Manthi, for their assistance with the rind thickness project and their invaluable friendship and support.

Jesse Kuzy, for helping with all manner of experimental preparation and cleanup.

The rest of the McGregor Lab: Jorge, Samiksha, and Alex, for all their help with my research, as well as our undergraduate workers, especially Ingrid, Erin, Taylor, and Jared.

Manoj Sapkota and Yasin Topcu, for their help with QTLseq, primer design, and figure design.

Dr. Scott Gold and Ben Averitt, for providing me with my first experiences with genetics research and plant breeding.

Dr. Caywood Chapman and Kim Wimpy, for inspiring a love of biology and plants in a very lost teenager.

TABLE OF CONTENTS

LIST OF TABLES

Page

LIST OF FIGURES

Page

CHAPTER 1

INTRODUCTION

By the year 2050 the population of earth is expected to exceed 9 billion people. Feeding this many people will require a massive increase in crop yields over current levels (Godfray et al. 2010). There are two obvious solutions to this problem. The first is to devote more and more land to agriculture. This is neither a wise or ethical option, on account of the massive effect that human beings have already had on the natural state of the world, and the precarious state our biosphere already finds itself in (Ceballos et al. 2015). It is a far more tenable idea to instead increase the amount of food that we can produce from the land that has already been devoted to agriculture. Given that around 20-40% of global agricultural productivity is lost annually to pathogens and other biotic factors, reducing losses due to pathogens should be a fruitful avenue for yield increases (Savary et al. 2012). Combating plant pathogens can primarily be done in three ways: cultural practices, which can be labor, and, therefore, cost intensive; chemical control, which is also expensive in addition to being potentially damaging to the environment, making it the least desirable option; and finally using resistant plant cultivars, which are expensive to develop but relatively cheap to deploy, with no increase in labor required by the growers (Hogenboom 1993). It is for these reasons that the development of resistant cultivars will be the most effective option for overall yield improvement, while simultaneously reducing anthropogenic environmental impacts. The development of these resistant cultivars is now aided and accelerated by the rapid pace of advancements in the fields of genetics, genomics, and bioinformatics, which have provided

an ever-expanding toolbox with which to manipulate life, and a continuous supply of new techniques to be applied to the myriad number of food crops grown on this planet.

Watermelon Origins and Taxonomy

While it was originally cultivated as a storable source of fresh clean water in arid climates, today watermelon is cultivated primarily for its sweet flesh, which is traditionally eaten fresh (Paris 2015). However, watermelon is also cultivated for its seeds, for pickling, or for making jams or preserves. (Nerson et al. 1994, Gusmini et al. 2004, Souad et al. 2012). Watermelon is a member of the *Cucurbitaceae* family, whose members include squashes, pumpkins, gourds, melons, and cucumbers. The sweet dessert fruit that consumers would recognize as watermelon is classified as *Citrullus lanatus* (Renner et al. 2017). The genus includes several other species: *Citrullus mucosospermus*, the egusi melon, which is cultivated for its seeds; *Citrullus amarus*, the citron melon, which is usually pickled or used to make fruit preserves; *Citrullus colocynthis*, the colocynth melon, which has traditionally been cultivated for it medicinal properties; *Citrullus ecirrhosus*, which is a tendril-less perennial closely related to *C. amarus; Citrullus rehmii*, an annual species endemic to the Namib; and *Citrullus naudinianus*, a perennial species with distinct raised points on its fruit (Renner et al. 2017).

Watermelon has been cultivated for at least 4,000 years, based on reports of seeds of *C. colocynthis* from Egyptian archeological remains containing seeds and fruit dating to around 4,500 and 4,000 years old respectively, with images thought to depict *C. lanatus* of a similar age also discovered in the same region (Paris 2015). Earlier evidence of *Citrullus* cultivation by humans comes in the form of *Citrullus* seeds found at Uan Muhuggiag, a Libyan archeologic site, which carbon dating showed to be over 6,000 years old (Wolcott et al. 2021). The species of these seeds could not be definitively determined, but they exhibited cracking patterns consistent with crushing

by human teeth. The earliest hard evidence of sweet watermelon that we have, comes in the form of photographs of seeds taken from the tomb of Tutankhamen, which would place the seeds at over 3,000 years old. Based on this, as well as the presence of wild-growing dessert type watermelon in northeastern Africa, and etymological studies of words used for various crops in ancient texts, it was proposed that the sweet dessert watermelon *C. lanatus* originated in northeastern Africa around 4,000 years ago (Paris 2015). This hypothesis was later corroborated by samples of Kordofan melon (*C. lanatus subsp. cordophanus*) collected in Sudan (Renner et al. 2021). These melons resemble what appear to be pictures of early cultivated *Citrullus* from archaeological sites, and sequencing data shows them to be the closest relative of cultivated watermelon.

Economic Importance

Watermelon is a globally important horticultural crop, with a global planting of over 3 million hectares, leading to an average global harvest of over 100 million tonnes annually (FAOSTAT Economic Data 2019). Despite being produced globally, the vast majority of the world's watermelon is grown in China, which produces over 60 million tonnes annually. The USA was ranked eighth globally for watermelon production in 2019, after China, Turkey, Iran, India, Kazakhstan, and Egypt, and produces around 1.5 million tonnes annually on around 41 thousand hectares. Within the USA, Georgia ranks third, behind California and Florida for watermelon production, producing between 500 and 600 million pounds of watermelon annually (FAOSTAT Economic Data 2019). In 2019 watermelon was planted on around 22,300 hectares in Georgia, primarily in the costal plain region, leading to a crop value of $180 million (2019 Farm Gate Value Report 2020). As these figures show, watermelon is not just an important global food crop, but an important part of the economy of the United States, and Georgia in particular.

Disease pressure has a large impact on the productivity of watermelon fields globally. In Georgia in the year 2019, disease was responsible for a 14% reduction in the watermelon crop value, a loss of $25.2 million. This was despite the expenditure of $8.1 million in attempt to control disease, primarily through the use of fungicides (Little 2020). Watermelon suffers from a variety of diseases including damping off, anthracnose, root knot nematodes, fusarium wilt, bacterial fruit blotch, downy mildew, and gummy stem blight. Of these diseases gummy stem blight (GSB) is one of the most damaging, due to a lack of resistant cultivars and recently developed fungicide resistance in some isolates (Li et al. 2016). While resistant cultivars have been developed for some diseases of watermelon, the lack of GSB-resistant cultivars keeps growers dependent on the broad-spectrum fungicides used to control GSB as well as a variety of other diseases. This prevents any economic gains from being made by deploying resistance to the many other pathogens which are effectively controlled by the fungicides used to control GSB (Wehner 2008, Egel 2012). Due to this, GSB resistance is essentially the keystone which would complete a pyramid of resistance genes to be deployed that could help to free growers from the economic burden of foliar fungicide applications and decrease the environmental impact of watermelon production.

Watermelon Breeding and Genetics

The initial plant selections that lead to the first domesticated varieties were performed inadvertently by hunter-gatherers, allowing agrarian civilization to arise (Diamond 2002). As civilization has grown and developed, so too has its ability to manipulate the nature of the crops that are grown. The discovery of DNA and the development of the tools to manipulate it, have led to a paradigm shift in the field of plant breeding, which had long relied entirely on indirect methods like phenotypic traits and crosses to track and manipulate the genetics of plants (Bernardo 2002). This necessitated growing large numbers of progeny at every stage of the process, often at great

cost to the breeder (Sedcole 1977). With advances in the field of genetics, breeders are now able to screen plants for desirable traits based on their genetic makeup, and even insert desirable genes into plants or delete undesirable genes (Birch 1997, Collard et al. 2005, Barrangou & Doudna 2016). This has allowed breeders to greatly increase their effectiveness by decreasing the number of undesirable plants which must be grown, as well as accomplish things that would have never been possible using conventional breeding, such as introducing the bacterial gene responsible for the production of the pesticide Bt to plant genomes (Hilder & Boulter 1999).

Watermelon cultivars can be divided into three categories: open-pollinated varieties; F_1 hybrids, which are varieties created by controlled crossing of two highly inbred lines to produce heterozygous progeny; and triploids, which are F_1 hybrids with the added benefit of having highly desirable "seedless" fruit (Wehner 2008). This seedless fruit contains only very small white seedcoats from aborted seed. This is due to the uneven number of chromosomes causing uneven pairing during miosis. While seedless watermelon is preferred by US consumers, the seed is also much more expensive, due to the more complex process required to create them. First, a diploid plant has its chromosomes doubled using a chemical such as colchicine or oryzalin to generate a tetraploid plant. The tetraploid plants are then pollinated with diploid pollen, resulting in triploid seeds (Kihara 1947). These triploid seeds are then planted and pollinized using a diploid pollinizer to generate seedless watermelon. Watermelon of this type makes up a majority of the market in the USA, where they are consumed for their flesh.

Genomic Tools for Watermelon

The selection of plants for desirable traits without phenotyping is accomplished through the use of various types of molecular markers. Types of molecular markers include restriction fragment length polymorphisms (RFLP), random amplified polymorphic DNA (RAPD), simple

sequence repeats (SSR), which are also called microsatellites-, amplified fragment length polymorphisms (AFLP), and single nucleotide polymorphisms (SNP). The older types of genetic markers utilize hybridization with fluorescent or radioactive probes, and/or amplification via the polymerase chain reaction (PCR) of various fragments of DNA to create patterns on electrophoresis gels. The patterns of these fragments are determined by the genotype of the sample and are used to look for traits or associations within a group of organisms (Jones et al. 1997). Newer, more efficient methods have been developed which instead rely on sequencing and genomic analysis to detect markers, eliminating the need to run and decipher large numbers of electrophoresis gels. With these sequencing-based methods, SNPs, which could not be readily detected by earlier methods, have become incredibly useful as markers (Rafalski 2002). Genetic markers allow us to build linkage maps of chromosomes, and locate genes within them, by observing recombination rates among markers to determine how closely linked they are to each other.

Next-generation sequencing technology has enabled the publication of two draft watermelon genomes. 97103, an elite Chinese variety, was the first to have a draft genome published (Guo et al. 2013). The published genome was made up of 353 million base pairs on 11 chromosomes and accounted for 83.2% of the estimated size of the genome. Annotation revealed 23,440 predicted genes. This was followed in 2015 by a draft genome for Charleston Gray, an elite American cultivar (Wu et al., 2019). The genome consists of 382 million base pairs across 11 chromosomes accounting for an estimated 96.16% of the genome. Annotation of this genome has revealed 22,567 predicated genes. These genomes can be of great benefit to watermelon breeders by allowing them to find candidate genes for their traits of interest. The 97103 genome was later

updated with a second version (Guo et al. 2019). This version contained 362 million base pairs over 11 chromosomes accounting for an 99.3% of the genome assembly.

Quantitative Trait Loci

Unlike the colored flowers of Mendel's pea plants, many plant traits, including some of the most desirable ones such as yield, exist as a continuous spectrum, controlled by many genes. These are called quantitative traits, and the areas within the genome which contain them are referred to as quantitative trait loci (QTL). The presence or absence of QTL in a DNA sample can be determined using closely linked molecular markers, segments of DNA near to, but distinct from the gene of interest, which exhibit polymorphisms that can be used to test for the presence of said gene (Collard et al. 2005). The identification of these QTL and associated markers is of great interest to plant breeders, as it allows them to rapidly screen plants for the presence or absence of alleles contributing to a key trait without conducting expensive phenotyping experiments at every step of the process. Using marker-assisted selection (MAS), seeds or seedlings are screened with molecular tests for markers linked to desirable genes. Only the individuals possessing the desired markers are planted for the next stage of the breeding program. The presence of desirable traits can be validated phenotypically at the end of the breeding process. This can lead to massive savings of time, resources, and field and glasshouse space for breeders. QTLs can be located using phenotypic data in combination with linkage maps, which use the recombination frequencies of DNA associated with genetic markers to determine the locations of and genetic distances between markers on the chromosome (Lander and Botstein 1989). This technique has been used in watermelon to identify QTL linked to traits including fruit length, diameter, and weight, rind thickness, flowering time, and gummy stem blight resistance (Sandlin et al. 2012, Gimode et al. 2019, 2021, Ren et al. 2019, Lee et al. 2021).

With the advent of high throughput sequencing technology and advances in bioinformatics, a method called QTL-seq was developed (Takagi et al. 2013). This method is based on earlier forms of bulk segregant analysis developed by Michelmore (1991). In QTL-seq two DNA bulks are constructed from the most phenotypically extreme individuals in a segregating population. These bulks are then sequenced using next-generation sequencing technology such as the Illumina platform. Specialized software is then used to compare the sequences from the two DNA bulks and identify segments of the genomes where the ratios of polymorphisms are significantly different between the two bulks (Mansfeld and Grumet 2018). The identified polymorphisms which have become highly segregated between the two bulks should in theory be tightly associated with the QTL of interest. The type of polymorphism most commonly used for this technique is known as a single nucleotide polymorphism or SNP and consists of a single base pair difference between a region in two different segments of DNA (Pierce 2014). This technique has been used in watermelon to map traits including *Fusarium* resistance, gummy stem blight resistance, and dwarfism (Dong et al. 2018, Fall et al. 2018, Ren et al. 2019)

Gummy Stem Blight

The first reports of gummy stem blight on a cucurbit came from Europe in 1869 from Auerwald and Fuckel who both, separately described a disease of the cucurbit *Bryonia*, and described it as *bryoniae*, although they both used different genera in their descriptions (Keinath 2011). It was first described as *Didymella bryoniae* by Rehm in 1881 and was known by that name for over 100 years (Index Fungorum). The disease was first described on watermelon in 1891 from infected watermelon plants in Delaware. In this publication the disease was described as a species of *Phylosticta* (Chester 1891). GSB has since been reported on cucurbit crops world-wide,

purportedly being spread by the movement of seeds and plant materials between cucurbit-producing regions (Keinath 2011).

Gummy stem blight was thought to be caused by a single species of fungus *Didymella bryoniae*, however it was recently discovered to be caused by a group of three morphologically identical species of fungi. *Didymella bryoniae* was renamed to *Stagonosporopsis cucurbitacearum* and placed into a genus along with *S. caricae* and *S. citrulli* (Stewart et al. 2015). These three *Stagonosporopsis* species all cause gummy stem blight and are ascomycete fungi. They are spread from field to field by wind-blown ascospores, which are sexually produced inside of flask-like structures called pseudothecia (Zitter et al. 1996). The disease can also be moved between fields on infected seeds or transplants, or by the agricultural activities of humans (Keinath 1996).

After landing on the plant, the ascospores germinate and proceed to penetrate the plants tissues, usually through a wound or natural openings, but direct penetration has also been reported (Schwartz & Gent 2007). After infection the plant develops dark brown or tan lesions, usually beginning at the margins of the leaves. On stems, the fungi can cause cankers which lead to wilting. Once an infection has been established, more pseudothecia, producing ascospores, as well as pycnidia, producing asexual conidia, are formed to spread the infection further. While the ascospores are produced in a mostly dry manner to facilitate wind dispersal, the conidia are produced and exuded within a gummy substance. This gives the disease its name. The gummy substance necessitates water splashing for dispersal of the conidia (Zitter et al. 1996). Spreading of the disease within a field is accomplished primarily via the conidia. Infection by the pathogen depends on high moisture conditions, with humidity and standing water on the leaves greatly enhancing the ability of the pathogen to infect plants. Previous studies have shown a temperature of 21-24°C to be ideal for infection of cucumber plants by the pathogen (Arny & Rowe 1991).

GSB Resistance in Watermelon

While much work has been devoted to finding GSB resistance in watermelon germplasm, little progress has been made in its introgression into elite cultivars. In 1962 GSB resistance was discovered in PI 189225 of the USDA germplasm collection as well as a few other accessions (Sowell & Pointer 1962). Boyhan et al. (1994) reported the screening of 138 PIs from the USDA germplasm collection for GSB resistance. The authors reported five highly resistant accessions. Screening of all available watermelon germplasm accessions from the USDA-ARS, identified 10 highly resistant lines, including PI 189225 and PI 526233 (Gusmini et al. 2005). Using resistant PIs reported by Sowell and Pointer (PI 189225 and PI 271778) as parents in crosses with elite cultivars, Norton et al. (1986, 1993, 1995) developed four cultivars (AU-Producer, AU-Golden Producer, AU-Jubilant, and AU-Sweet Scarlet) purported to exhibit moderate resistance to GSB. Unfortunately, these cultivars did not perform as well in actual growing conditions as was reported in the trials (Gusmini et al. 2005). Norton's development of the purported "resistant" cultivars was conducted under the assumption that GSB resistance was conferred by a single recessive gene, *db*, from PI 189225 (Norton 1979). However, Gusmini et al. (2017) demonstrated that the segregation ratios in several crosses were not consistent with Norton's hypothesis. Gusmini et al. (2017) hypothesized that GSB resistance is controlled by many quantitative genes, and that their identification is being made difficult by the large contributions of environmental factors to GSB development. In light of the recent discovery that GSB is caused by a group of three *Stagonosporopsis* species, rather than a single species of *Didymella*, it is hypothesized that the difficulty locating and introgressing GSB resistance into elite lines is also exacerbated by differential levels of virulence among species, and differences in pathogenicity between species and different cultivars (Gimode et al., 2020). The cultivars developed by Norton et al. (1986, 1993,

1995) were screened with a single or very few isolates and it is unknown to which *Stagonosporopsis* species they belonged. It is highly unlikely that they constituted a representative sample of the *Stagonosporopsis* genetic diversity known to be responsible for causing GSB.

Previously Identified Resistance QTL

GSB resistance QTL in watermelon have been described in three studies. A GSB resistance QTL on chromosome eight was identified by Ren et al. (2019) using a population derived from K3 (*C. lanatus*) × PI 189225 (*C. amarus*), screened with an isolate of *S. cucurbitacearum*. Lee et al. (2021) mapped three "*D. bryoniae* 'KACC 40937 isolate" resistance QTL, one on chromosome six and two on chromosome eight, using a population derived from 920533 (*C. lanatus*) × PI 189225. The QTL mapped on chromosome 8 by the two studies do not co-localize. The species of *Stagonosporopsis* used by Lee et al (2021) is not known. Gimode et al. (2021) used a population derived from Crimson Sweet (*C. lanatus*) × PI 482276 (*C. amarus*) and *S. citrulli* isolate 12178A to map resistance QTL on chromosomes 5 and 7. Differences in the locations of these QTL, especially those derived from the same resistant parent (PI 189225), are likely due to either differences in resistance to the various species or isolates of *Stagonosporopsis* used for phenotyping or differences in phenotyping methodologies. Lee et al. (2021) evaluated stem lesions and leaf lesions separately, while Ren et al. (2019) scored only leaf lesions, and Gimode et al. (2021) scored the entire seedling. These QTL had PVE values ranging from 6.4% to 32% demonstrating a need for a pyramid of multiple genes to achieve a desirable level of resistance.

Rind Thickness

Traditionally the availability of watermelon, like most other perishable fruit, was limited to a short period of time following the harvest in a given location. Modern society has advanced from this system to one in which packaging and shipping technologies allow many fruit to be

available year round thanks to growers in many different regions each being able to fill the needs of the global market following its harvest season. However, such long-distance shipping demands a watermelon that can withstand the rigors of shipping, with watermelons often being stacked on top of one another in large shipping bins. This durability is primarily influenced by two factors. Durable rind (*E*) has been shown to be dominant to exploding rind (*e*) (Porter 1937, Poole 1944). Fruit with the exploding rind trait are prone to cracking and breaking, making them unsuitable for shipping, but useful as easily crushed pollenizers (Wehner 2012). Shipping durability has also been shown to be improved in watermelons possessing a thicker rind (Sadrnia et al. 2009). While this would seem to make a very thick rind the ideal phenotype, this shipping durability must be balanced against consumer preference, which demands that the rind make up a relatively small portion of the overall fruit diameter (FD) (Wehner 2008).

In order to help balance these two needs, it would be beneficial to have a functional understanding of the loci controlling rind thickness (RTH), along with closely linked markers so these regions can be tracked in breeding populations. Two such QTL have been identified: *QFD2.2* is a fruit diameter (FD) QTL which overlaps with a RTH QTL, and *QRTH5.1*. is a minor unvalidated QTL associated with RTH, but not other fruit traits (Sandlin et al. 2012, Yang et al. 2021). Sandlin et al. (2012) used a population derived from Klondike Black Seed (*C. lanatus*) × New Hampshire Midget (*C. lanatus*) (KxN) and Yang et al. (2021) used a population derived 1061 (*C. lanatus*) × 812 (*C. lanatus*).

RTH has been shown to be positively correlated with fruit weight (FWT), fruit length (FL) and fruit diameter (Sandlin et al. 2012, Yang et al. 2021). In one study, *QFD2.2* was shown to overlap with QTL controlling FWT and RTH in addition to FD (Sandlin et al. 2012). Later work has mapped a QTL associated with FD in the same location but did not collect data for RTH (Cheng

et al. 2016). Sandlin et al. (2012) also mapped major QTL controlling FL on chromosome three. Later studies also mapped this QTL in different genetic backgrounds, and posited *Cla011257* (*ClSUN25-26-27a*) as the putative candidate gene responsible for the effect on FL (Kim et al. 2015, Liu et al. 2016, Pan et al. 2017, 2020, Dou et al. 2018). *Cla011257* is an ortholog (*ClSUN25-26-27a*) of SUN, a gene known to control fruit shape in tomato by increasing the amount of cell division occurring along the proximal-distal fruit axis (Wu et al. 2011, Pan et al. 2020). There are three known alleles of this gene in watermelon: the wild type (WT) which is associated with round fruit; a 159bp deletion (DEL) associated with elongated type fruit such as those of "Charleston Gray"; and a G to A point mutation (KBS) which is associated with the intermediate phenotype of "Klondike Black Seed"(Legendre et al. 2020, Pan et al. 2020). This gene is the likely long ago hypothesized *O* gene controlling fruit shape (Weetman 1937, Tanaka et al. 1995, Pan et al. 2020).

Aims of the Study

(1) Use QTL-seq to identify QTL associated with GSB resistance in a mapping population derived from Sugar Baby and PI 189225, using an isolate of *S. citrulli,* and develop KASP marker assays for selection of these loci. This will add to the body of evidence generated by previous studies to help elucidate resistance loci to the various species and isolates of GSB causing *Stagonosporopsis*. Additionally, the marker assays would allow breeders to introgress resistance loci into commercial watermelon germplasm for use by farmers, potentially in a pyramid with other resistance QTL.

(2) Validate *QRTH5.1* as a significant contributor to rind thickness in watermelon and determine the role of fruit size (*QFD2.2)* and shape (*QFSI3.1)* QTL on rind thickness. This will help breeders to better understand the mechanism controlling rind thickness in

watermelon, allowing more granular and intentional control of rind thickness to satisfy both the rigors of shipping and the demands of a modern consumer.

References

2019 Farm Gate Value Report. 2020. University of Georgia Center for Agribusiness and Economic Development.

Arny, C.J. and R.C. Rowe. 1991. Effects of temperature and duration of surface wetness on spore production and infection of cucumbers by *Didymella bryoniae*. Phytopathology 81:206–209.

Barrangou, R. and J.A. Doudna. 2016. Applications of CRISPR technologies in research and beyond. Nat Biotechnol. 34:933–941.

Bernardo, R.N. 2002. Breeding for quantitative traits in plants. Third edition, Stemma Press, Woodbury, Minnesota.

Birch, R.G. 1997. Plant Transformation: Problems and Strategies for Practical Application. Annual Review of Plant Physiology and Plant Molecular Biology 48:297–326.

Boyhan, G., J. Norton and B. Abrahams. 1994. Screening for resistance to anthracnose (race 2), gummy stem blight, and root knot nematode in watermelon germplasm. Cucurbit Genetics Cooperative Report 17:106–110.

Ceballos, G., P.R. Ehrlich, A.D. Barnosky, A. García, R.M. Pringle and T.M. Palmer. 2015. Accelerated modern human–induced species losses: Entering the sixth mass extinction. Science Advances 1:e1400253.

Cheng, Y., F. Luan, X. Wang, P. Gao, Z. Zhu, S. Liu, A.M. Baloch and Y. Zhang. 2016. Construction of a genetic linkage map of watermelon (*Citrullus lanatus*) using CAPS and SSR markers and QTL analysis for fruit quality traits. Scientia Horticulturae 202:25–31.

Chester, F.D. 1891. Notes on three new or noteworthy diseases of plants. Bulletin of the Torrey Botanical Club 18:371–374.

Collard, B.C.Y., M.Z.Z. Jahufer, J.B. Brouwer and E.C.K. Pang. 2005. An introduction to markers, quantitative trait loci (QTL) mapping and marker-assisted selection for crop improvement: The basic concepts. Euphytica 142:169–196.

Diamond, J. 2002. Evolution, consequences and future of plant and animal domestication. Nature 418:700–707.

Dong, W., D. Wu, G. Li, D. Wu and Z. Wang. 2018. Next-generation sequencing from bulked segregant analysis identifies a dwarfism gene in watermelon. Scientific Reports 8:2908.

Dou, J., S. Zhao, X. Lu, N. He, L. Zhang, A. Ali, H. Kuang and W. Liu. 2018. Genetic mapping reveals a candidate gene (*ClFS1*) for fruit shape in watermelon (*Citrullus lanatus* L.). Theor Appl Genet 131:947–958.

Egel, D. 2012. Muskmelon and watermelon fungicide guide for Indiana 2012.

Fall, L.A., J. Clevenger and C. McGregor. 2018. Assay development and marker validation for marker assisted selection of *Fusarium oxysporum* f. sp. *niveum* race 1 in watermelon. Mol. Breeding 38:130.

FAOSTAT. 2020. FAOSTAT Crop Production Data. 1 August 2020. <http://www.fao.org/faostat/en/>

Gimode, W., K. Bao, Z. Fei and C. McGregor. 2021. QTL associated with gummy stem blight resistance in watermelon. Theor. Appl. Genet. 134:573–584.

Gimode, W., J. Clevenger and C. McGregor. 2019. Fine-mapping of a major quantitative trait locus *Qdff3-1* controlling flowering time in watermelon. Mol. Breeding 40:3.

Godfray, H.C.J., J.R. Beddington, I.R. Crute, L. Haddad, D. Lawrence, J.F. Muir, J. Pretty, S. Robinson, S.M. Thomas and C. Toulmin. 2010. Food security: the challenge of feeding 9 billion people. Science 327:812–818.

Guo, S., J. Zhang, H. Sun, J. Salse, W.J. Lucas, H. Zhang, Y. Zheng, L. Mao, Y. Ren, Z. Wang, J. Min, X. Guo, F. Murat, B.-K. Ham, Z. Zhang, S. Gao, M. Huang, Y. Xu, S. Zhong, A. Bombarely, L.A. Mueller, H. Zhao, H. He, Y. Zhang, Z. Zhang, S. Huang, T. Tan, E. Pang, K. Lin, Q. Hu, H. Kuang, P. Ni, B. Wang, J. Liu, Q. Kou, W. Hou, X. Zou, J. Jiang, G. Gong, K. Klee, H. Schoof, Y. Huang, X. Hu, S. Dong, D. Liang, J. Wang, K. Wu, Y. Xia, X. Zhao, Z. Zheng, M. Xing, X. Liang, B. Huang, T. Lv, J. Wang, Y. Yin, H. Yi, R. Li, M. Wu, A. Levi, X. Zhang, J.J. Giovannoni, J. Wang, Y. Li, Z. Fei and Y. Xu. 2013. The draft genome of watermelon (*Citrullus lanatus*) and resequencing of 20 diverse accessions. Nature Genetics 45:51–58.

Guo, S., S. Zhao, H. Sun, X. Wang, S. Wu, T. Lin, Y. Ren, L. Gao, Y. Deng, J. Zhang, X. Lu, H. Zhang, J. Shang, G. Gong, C. Wen, N. He, S. Tian, M. Li, J. Liu, Y. Wang, Y. Zhu, R. Jarret, A. Levi, X. Zhang, S. Huang, Z. Fei, W. Liu and Y. Xu. 2019. Resequencing of 414 cultivated and wild watermelon accessions identifies selection for fruit quality traits. Nat Genet 51:1616–1623.

Gusmini, G., L.A. Rivera-Burgos and T.C. Wehner. 2017. Inheritance of resistance to gummy stem blight in watermelon. HortScience 52:1477–1482.

Gusmini, G., J.R. Schultheis and T.C. Wehner. 2004. Rind thickness of watermelon cultivars for use in pickle production. HortTechnology 540–545.

Gusmini, G., R. Song and T.C. Wehner. 2005. New sources of resistance to gummy stem blight in watermelon. Crop Science 45:582–588.

Hogenboom, N.G. 1993. Economic importance of breeding for disease resistance, p. 5–9. *In* Durability of Disease Resistance, Current Plant Science and Biotechnology in Agriculture. Springer Netherlands, Dordrecht.

Index Fungorum. Entry for Didymella bryoniae. 5 Feb. 2019. <http://www.indexfungorum.org/names/NamesRecord.asp?RecordID=224305>

Jones, N., H. Ougham and H. Thomas. 1997. Markers and mapping: we are all geneticists now. The New Phytologist 137:165–177.

Keinath, A.P. 1996. Spread of *Didymella bryoniae* from contaminated watermelon seeds and transplants in greenhouse and field environments. Recent Research Developments in Plant Pathology 1:65–72.

Keinath, A.P. 2011. From native plants in central Europe to cultivated crops worldwide: the emergence of *Didymella bryoniae* as a cucurbit pathogen. HortScience 46:532–535.

Kihara, H. 1947. An application of sterility of autotriploids to the breeding of seedless watermelons. Seiken Ziho. 3:93–103.

Kim, K.-H., J.-H. Hwang, D.-Y. Han, M. Park, S. Kim, D. Choi, Y. Kim, G.P. Lee, S.-T. Kim and Y.-H. Park. 2015. Major quantitative trait loci and putative candidate genes for powdery mildew resistance and fruit-related traits revealed by an intraspecific genetic map for watermelon (*Citrullus lanatus* var. *lanatus*). PLOS ONE 10:e0145665.

Lander, E.S. and D. Botstein. 1989. Mapping mendelian factors underlying quantitative traits using RFLP linkage maps. Genetics 121:185–199.

Lee, E.S., D.-S. Kim, S.G. Kim, Y.-C. Huh, C.-G. Back, Y.-R. Lee, M.I. Siddique, K. Han, H.-E. Lee and J. Lee. 2021. QTL mapping for gummy stem blight resistance in watermelon (*Citrullus spp.*). Plants 10:500.

Li, H.-X., T.A. Nuckols, D. Harris, K.L. Stevenson and M.T. Brewer. 2019. Differences in fungicide resistance profiles and multiple resistance to a quinone-outside inhibitor (QoI), two succinate dehydrogenase inhibitors (SDHI), and a demethylation inhibitor (DMI) for two *Stagonosporopsis* species causing gummy stem blight of cucurbits. Pest Management Science 75:3093–3101.

Little, E. 2020. 2019 Georgia plant disease loss estimates. University of Georgia Cooperative Extension.

Liu, S., P. Gao, Q. Zhu, F. Luan, A.R. Davis and X. Wang. 2016. Development of cleaved amplified polymorphic sequence markers and a CAPS-based genetic linkage map in watermelon (*Citrullus lanatus* [Thunb.] Matsum. and Nakai) constructed using whole-genome re-sequencing data. Breeding Science 66:244–259.

Mansfeld, B.N. and R. Grumet. 2018. QTLseqr: an R package for bulk segregant analysis with next-generation sequencing. The Plant Genome 11.

Michelmore, R.W., I. Paran and R.V. Kesseli. 1991. Identification of markers linked to disease-resistance genes by bulked segregant analysis: a rapid method to detect markers in specific genomic regions by using segregating populations. PNAS 88:9828–9832.

Nerson, H., Y. Burger and R. Berdugo. 1994. High plant density and irrigation increase watermelon yield grown for seed consumption. Advances in Horticultural Science 8:101–105.

Norton, J.D. 1979. Inheritance of resistance to gummy stem blight [caused by *Didymella bryoniae*] in watermelon. HortScience (USA) 14:630–632.

Norton, J.D., G.E. Boyhan, D.A. Smith and B.R. Abrahams. 1993. “AU-Golden Producer” watermelon. HortScience 26:681–682.

Norton, J.D., G.E. Boyhan, D.A. Smith and B.R. Abrahams. 1995. “AU-Sweet Scarlet” watermelon. HortScience 30:393–394.

Norton, J.D., R.D. Cosper, D.A. Smith and K.S. Rymal. 1986. “AU-Jubilant” and “AU-Producer” watermelons. HortScience (USA) 21:1460–1461.

Pan, Y., X. Liang, M. Gao, H. Liu, H. Meng, Y. Weng and Z. Cheng. 2017. Round fruit shape in WI7239 cucumber is controlled by two interacting quantitative trait loci with one putatively encoding a tomato SUN homolog. Theor. Appl. Genet. 130:573–586.

Pan, Y., Y. Wang, C. McGregor, S. Liu, F. Luan, M. Gao and Y. Weng. 2020. Genetic architecture of fruit size and shape variation in cucurbits: a comparative perspective. Theor. Appl. Genet. 133:1–21.

Paris, H.S. 2015. Origin and emergence of the sweet dessert watermelon, *Citrullus lanatus*. Ann Bot 116:133–148.

Rafalski, A. 2002. Applications of single nucleotide polymorphisms in crop genetics. Current Opinion in Plant Biology 5:94–100.

Ren, R., J. Xu, M. Zhang, G. Liu, X. Yao, L. Zhu and Q. Hou. 2019. Identification and molecular mapping of a gummy stem blight resistance gene in wild watermelon (*Citrullus amarus*) germplasm PI 189225. Plant Disease 104:16–24.

Renner, S.S., A. Sousa and G. Chomicki. 2017. Chromosome numbers, Sudanese wild forms, and classification of the watermelon genus *Citrullus*, with 50 names allocated to seven biological species. Taxon 66:1393–1405.

Renner, S.S., S. Wu, O.A. Pérez-Escobar, M.V. Silber, Z. Fei and G. Chomicki. 2021. A chromosome-level genome of a Kordofan melon illuminates the origin of domesticated watermelons. PNAS 118.

Sadrnia, H., A. Rajabipour, A. Jafari, A. Javadi, Y. Mostoufi, T. Bagherpour and N.M. Khojasteh. 2009. Mechanical failure of two varieties of watermelon under quasi static load. Iranian Journal of Biosystems Engineering 40:169–174.

Sandlin, K., J. Prothro, A. Heesacker, N. Khalilian, R. Okashah, W. Xiang, E. Bachlava, D.G. Caldwell, C.A. Taylor, D.K. Seymour, V. White, E. Chan, G. Tolla, C. White, D. Safran, E. Graham, S. Knapp and C. McGregor. 2012. Comparative mapping in watermelon [*Citrullus lanatus* (Thunb.) Matsum. et Nakai]. Theor. Appl. Genet. 125:1603–1618.

Savary, S., A. Ficke, J.-N. Aubertot and C. Hollier. 2012. Crop losses due to diseases and their implications for global food production losses and food security. Food Sec. 4:519–537.

Schwartz, H.F. and D.H. Gent. 2007. Gummy stem blight and black rot (cucumber, melon, pumpkin, squash, and zucchini). *In* High Plains IPM Guide. Cooperative effort of the University of Wyoming, University of Nebraska, Colorado State University and Montana State University.

Sedcole, J.R. 1977. Number of Plants Necessary to Recover a Trait. Crop Science.

Souad, A.M., P. Jamal and K.S. Olorunnisola. 2012. Effective jam preparations from watermelon waste.

Sowell, G. and G.R. Pointer. 1962. Gummy stem blight resistance of introduced watermelons.

Stewart, J.E., A.N. Turner and M.T. Brewer. 2015. Evolutionary history and variation in host range of three *Stagonosporopsis* species causing gummy stem blight of cucurbits. Fungal Biology 119:370–382.

T. A Zitter, D.L. Hopkins and C.E. Thomas. 1996. Compendium of cucurbit diseases, Disease compendium series. APS Press, St. Paul, Minn.

Takagi, H., A. Abe, K. Yoshida, S. Kosugi, S. Natsume, C. Mitsuoka, A. Uemura, H. Utsushi, M. Tamiru, S. Takuno, H. Innan, L.M. Cano, S. Kamoun and R. Terauchi. 2013. Qtl-seq: rapid mapping of quantitative trait loci in rice by whole genome resequencing of DNA from two bulked populations. The Plant Journal 74:174–183.

Wehner, T.C. 2008. Watermelon, p. 381–418. *In* J. Prohens & F. Nuez (eds.). Vegetables I: Asteraceae, Brassicaceae, Chenopodicaceae, and Cucurbitaceae, Handbook of Plant Breeding. Springer New York, New York, NY.

Winter, P. and G. Kahl. 1995. Molecular marker technologies for plant improvement. World Journal of Microbiology & Biotechnology 11:438–448.

Wolcott, K.A., G. Chomicki, Y.M. Staedler, K. Wasylikowa, M. Nesbitt, J. Schönenberger and S.S. Renner. 2021. Three-dimensional X-ray-computed tomography of 3300- to 6000-year-old Citrullus seeds from Libya and Egypt compared to extant seeds throws doubts on species assignments. Plants, People, Planet.

Wu, S., X. Wang, U. Reddy, H. Sun, K. Bao, L. Gao, L. Mao, T. Patel, C. Ortiz, V.L. Abburi, P. Nimmakayala, S. Branham, P. Wechter, L. Massey, K.-S. Ling, C. Kousik, S.A. Hammar, Y. Tadmor, V. Portnoy, A. Gur, N. Katzir, N. Guner, A. Davis, A.G. Hernandez, C.L. Wright, C. McGregor, R. Jarret, X. Zhang, Y. Xu, T.C. Wehner, R. Grumet, A. Levi and Z. Fei. 2019. Genome of 'Charleston Gray', the principal American watermelon cultivar, and genetic characterization of 1,365 accessions in the U.S. National Plant Germplasm System watermelon collection. Plant Biotechnology Journal 17:2246–2258.

Wu, S., H. Xiao, A. Cabrera, T. Meulia and E. van der Knaap. 2011. *SUN* regulates vegetative and reproductive organ shape by changing cell division patterns. Plant Physiology 157:1175–1186.

Yang, S.-L. and T.W. Walters. 1992. Ethnobotany and the economic role of the cucurbitaceae of china. Econ Bot 46:349–367.

Yang, T., S. Amanullah, J. Pan, G. Chen, S. Liu, S. Ma, J. Wang, P. Gao and X. Wang. 2021. Identification of putative genetic regions for watermelon rind hardness and related traits by BSA-seq and QTL mapping. Euphytica 217:19.

CHAPTER 2

QTL ASSOCIATED WITH RESISTANCE TO *STAGONOSPOROPSIS CITRULLI* IN *CITRILLUS AMARUS*[1]

[1]Adams, L. and McGregor, C. To be submitted.

Abstract

Gummy stem blight (GSB) is a fungal disease affecting cucurbit crops, including watermelon (*Citrullus lanatus*), leading to significant yield losses. The disease is caused by three *Stagonosporopsis* species, of which *S. citrulli* is the most common in the southeastern United States. Currently no gummy stem blight-resistant watermelon cultivars are available to growers. In this study we used QTL-seq in an interspecific population developed from Sugar Baby × PI 189225 (*C. amarus*) to identify a novel QTL associated with resistance to *S. citrulli* (PVE = 13.3%) on chromosome 5 (*Qgsb5.2*) of the watermelon genome. KASP marker assays were developed for selection of *Qgsb5.2* to allow breeders to track the allele contributing resistance to GSB, reducing the need for laborious phenotyping. Pyramiding different GSB resistance QTL could be a useful strategy to develop GSB resistant watermelon cultivars.

Keywords: Watermelon, *Citrullus lanatus*, *Citrullus amarus*, Gummy Stem Blight, *Stagonosporopsis citrulli*, Resistance, QTLseq, QTL Mapping.

Introduction

Gummy stem blight (GSB) is a fungal disease which affects cucurbit crops globally, leading to decreases in yield and revenue loss for growers (Keinath 2011, Stewart et al. 2015). Watermelon (*Citrullus lanatus*) is one of the most severely affected crops with average yield losses of up to 43% in unsprayed plots (Keinath & Duthie 1998). Until recently it was believed that GSB was caused by a single pathogen, *Didymella bryoniae*. However, Stewart et al (2015) determined that GSB is caused by three distinct species of *Stagonosporopsis*, *S. cucurbitacearum, S. caricae* and *S. citrulli*. Currently, GSB is controlled using costly fungicides that are damaging to the environment (Schwartz & Gent 2007, Wightwick et al. 2010), highlighting the need for resistant cultivars.

Initial efforts to breed watermelon with GSB resistance were conducted working under the hypothesis that the resistance in PI 189225 (*C. amarus*) was controlled by a single gene, designated *db* (Norton 1979). Norton used two resistant accessions, PI 189225 and PI 271778 (*C. lanatus*), to develop four cultivars ('AU-Producer', 'AU-Jubilant', 'AU-Sweet Scarlet', and 'AU-Golden Producer') with reported GSB resistance (Norton et al. 1986, 1993, 1995). Unfortunately, these varieties did not exhibit the same level of GSB resistance once they were grown by producers on a larger scale (Sumner & Hall 1993). Additional sources of GSB-resistant watermelon germplasm have been identified by other researchers in recent years (Boyhan et al. 1994, Song et al. 2004, Gusmini et al. 2005); however, to date, none of these discoveries have led to the release of GSB-resistant commercial watermelon cultivars. Recently, Gusmini et al. (2017) demonstrated that GSB resistance in four crosses between elite watermelon cultivars and resistant PIs, including PI 198225, is quantitatively inherited.

In three previous studies, researchers identified GSB resistance QTL in watermelon. Ren et al. (2019) used a population derived from K3 (*C. lanatus*) × PI 189225 and an isolate of *S. cucurbitacearum* to map a GSB resistance QTL on chromosome 8. Lee et al. (2021) used a population derived from 920533 (*C. lanatus*) × PI 189225 and "*D. bryoniae* 'KACC 40937 isolate'" to map GSB resistance QTL, two on chromosome 8 and one on chromosome 6. The QTL mapped by the two studies on chromosome 8 are distinct from one another. The species of *Stagonosporopsis* used by Lee et al (2021) is unknown. Gimode et al. (2021) used a population derived from Crimson Sweet (*C. lanatus*) × PI 482276 (*C. amarus*) and *S. citrulli* isolate 12178A to map GSB resistance QTL on chromosomes 5 and 7. Differences in the locations of these QTL, especially those derived from the same resistant parent (PI 189225), are likely due to either differences in resistance to the various species or isolates of *Stagonosporopsis* used for phenotyping or differences in phenotyping methodologies. Lee et al. (2021) evaluated lesion severity on the stems separately from leaf lesions, while Ren et al. (2019) scored only leaf lesions and Gimode et al. (2021) scored the entire seedling.

QTL-seq, a modification of bulked segregant analysis (Michelmore et al. 1991), was proposed by Takagi et al. (2013) as a quick and relatively cheap method to identify QTL associated with a particular trait. This technique has been widely used to identify QTL for various traits, including blast resistance in rice (Takagi et al. 2013), late spot resistance in peanut (Clevenger et al. 2018), and Fusarium wilt and GSB resistance in watermelon (Branham et al. 2018, Fall et al. 2018, Ren et al. 2019, Gimode et al. 2021, Lee et al. 2021).

The aim of the current study was to use QTL-seq to identify loci associated with resistance to *S. citrulli*, the most common GSB-causing *Stagonosporopsis* species in the southeastern US (Stewart et al. 2015), in a population derived from a cross between Sugar Baby (SB, susceptible)

and PI 189225 (resistant) and to develop KASP marker assays for selection of resistance loci in watermelon.

Materials and Methods

Plant Materials

A cross was made between Sugar Baby (*C. lanatus*, susceptible) and PI-189225 (*C. amarus*, resistant) and a single plant from the resulting F_1 was selfed to generate F_2 seed. F_2 plants were selfed in the greenhouse to produce 111 $F_{2:3}$ families. Leaf material collected from the parents, F_1 and F_2 plants were stored at -80 °C until use.

Inoculum Preparation

Stagonosporopsis citrulli isolate 12178A (provided by M. Brewer, collected in Berrien County, Georgia, U.S.A in 2012) was grown on full strength potato dextrose agar (PDA) for four weeks and then subcultured on quarter-strength PDA for a further 17 days. Conidia was harvested by flooding each Petri dish with 10 mL 0.1% Tween-20 (MilliporeSigma, St. Louis, MO) and scraping the plate with a microscope slide. The solution was filtered through 3 layers of cheese cloth and conidia were quantified under a microscope using a hemocytometer (Hausser Scientific, Horsham, PA). The conidial solution was diluted to 500,000 conidia per mL prior to inoculation. Due to low yields, a concentration of 420,000 conidia per mL was used for the re-screen.

Resistance Screening

Initial resistance screening was conducted between March 20th and April 8th, 2019, in a greenhouse in Athens, GA. Seed from the parents, F_1 and 111 $F_{2:3}$ families were sown in 48-well seedling trays in a randomized complete block design with four plants per block and four blocks. Two additional trays containing controls and 12 of the $F_{2:3}$ families were also sown for mock inoculations. Seedlings were grown in a greenhouse with supplemental lighting until the 2-3 true

leaf stage (16 days) and inoculated by spraying inoculum on the seedlings with a hand spray bottle until run-off. The mock inoculations were sprayed with 0.1% Tween-20 solution. After inoculation, the plants were placed inside a plastic tunnel with two humidifiers (Trion IAQ, Sanford, NC) in the greenhouse (average temperature = 24.0 °C, average humidity = 98.8%). After 72 hours, the seedlings were moved to a greenhouse bench and overhead watered twice per day for four days. At 7 days post inoculation, the seedlings were rated for disease severity using a 0-10 scale (0: no lesions present on the first two true leaves, 1: 1-10% of first two true leaves covered in lesions, 2: 11-20% of first two true leaves covered in lesions, 3: 21-30% of first two true leaves covered in lesions, 4: 31-40% of first two true leaves covered in lesions, one leaf beginning to collapse, 5: 40-50% of first two true leaves covered in lesions, 1 true leaf collapsed, 6: 1 of first two true leaves dead, other 1-25% of true leaves covered in lesions, 7: 1 of first two true leaves dead, other 26-50% covered in lesions, 8: 1 of first two true leaves dead, other 51-75% covered in lesions, 9: both first two true leaves dead, 10: seedling totally collapsed or dead). The mean severity rating for each family/control was calculated using JMP® version 15.0.0 (SAS Institute Inc., Cary, NC). A Shapiro-Wilk test was conducted using JMP to test the normality of the phenotypic distribution. The 20 most resistant and 20 most susceptible families were re-screened using the same protocol between May 1st and May 25th, 2019 (average temperature = 23.4 °C, average humidity = 91.7%). The 12 most resistant and most susceptible families over both screens were used to construct the bulks for QTL-seq.

DNA Extraction and Sequencing.

Frozen leaf material from the F_2 plants of the 24 selected $F_{2:3}$ families was ground using a TissueLyser II (QIAGEN, Hilden, Germany) and DNA was extracted using the E.Z.N.A. HP Plant DNA Mini Kit (Omega Bio-Tek Inc., Norcross, GA). DNA was quantified with an Infinite M200

Pro plate reader (Tecan Group Ltd., Mannedorf, Switzerland) using the i-control software (Tecan Group Ltd.,) and a NanoQuant Plate™ (Tecan Group Ltd.,). Agarose gel electrophoresis was used to confirm the quality of genomic DNA. Equal amounts of DNA from the 12 most resistant and 12 most susceptible families were pooled to create the resistant (R-Bulk) and susceptible bulk (S-Bulk), respectively. The samples were sent to Novogene (Novogene Corporation Inc., Davis, CA) for whole genome sequencing on an Illumina Platform (PE150, Q30>80%).

QTL-seq.

The raw reads were combined into forward and reverse read files for each bulk and checked for quality using FastQC (Andrews 2010). The reads were then aligned to the *C. lanatus* 97103_v2 (Guo et al. 2019) genome using BWA-MEM (Li 2013). The resulting SAM files were converted into BAM files using SAMtools (Li et al. 2009), which was also used to sort the reads by alignment position and then index the resulting BAM files. SAMtools was used to calculate mapping and pairing ratios of raw reads. BEDtools (Quinlan & Hall 2010) was then used to calculate average read depth for the BAM files. Read group names were standardized using Picard Tools (http://broadinstitute.github.io/picard/), which was then used to mark duplicate reads and index the files. SAMtools was used to index the 97103_v2 genome, and Picard Tools was used to create a dictionary file for the 97103_v2 genome. Reads were re-aligned using GATK (McKenna et al. 2010) to generate clean reads from misaligned regions. GATK was used to perform variant calling and the resulting VCF files from each bulk were combined into a single VCF file. GATK was used to filter the VCF file so that only SNPs remained. These SNPs were then filtered using GATK (QD < 2.0 || FS > 60.0 || MQ < 40.0 || MQRankSum < -12.5 || ReadPosRankSum < -8.0), and filtered SNPs were then removed using VCFtools (Danecek et al. 2011). GATK was used to output the SNPs from the VCF file into a table format suitable for use in the R (R Core Team & others

2013) package QTLseqr (Mansfeld & Grumet 2018). After importation into QTLseqr, SNPs were again filtered (refAlleleFreq = 0.2, minTotalDepth = 100, maxTotalDepth = 150, minSampleDepth = 40, minGQ =99), and then used to calculate the Δ-SNP index at each SNP (Takagi et al. 2013). This Δ-SNP index was used with a 1Mb sliding window to calculate a smoothed Δ-SNP index as well as 95% and 99% confidence intervals for a region's contribution to the trait of interest (GSB resistance).

Primer Design and Genotyping.

KASP (LGC Genomics LLC, Teddington, UK) primers were designed for SNPs spanning the regions of interest identified by QTLseqr using Primer3Plus and the *C. lanatus* 97103_v2 genome (Guo et al. 2019). DNA was extracted for parents, F_1, and all F_2 plants as previously described. KASP PCR reactions contained 1.94 μL of 2 × KASP Master Mix (LGC Genomics LLC), 0.06 μL of KASP Primer Mix, and 2 μL of DNA (10-20 ng/μl) in a total volume of 4 μL. The KASP Primer Mix contained 12 μL of each forward primer (100 μM), 30 μL of reverse primer (100 μM), and 46 μL of sterile distilled water. The following PCR conditions were used: 95°C for 15 minutes followed by 10 touchdown cycles of 95°C for 20 seconds, 66 °C for 25 seconds, and 72°C for 15 seconds, followed by 35 cycles of 95°C for 10 seconds, 57 °C for 60 seconds and 72°C for 15 seconds. KASP fluorescent end readings were measured using an Infinite M200 Pro (Tecan Group Ltd.) plate reader using the Magellan (Tecan Group Ltd.) software. Genotypes were called using KlusterCaller™ (LGC Genomics LLC).

QTL Mapping.

A genetic map (n = 111) was created of each region of interest using the following settings in ICIMapping (Meng et al. 2015): Grouping was performed by recombination frequency with a threshold value of 0.30, ordering was performed k-Optimally by recombination frequency using

the 2-OptMAP algorithm with 10 NN initials, rippling was performed by recombination frequency with a window size of 5. Resulting genetic maps were visualized using MapChart (Voorrips 2002). The genetic map was then used for QTL mapping using ICIMapping (Meng et al. 2015) with the following settings: The ICIM-ADD mapping method was used with deletion of missing phenotypes, a 1cM step, and a value of 0.001 for the probability in stepwise regression. The LOD threshold of 2.5079 was determined by running 1000 permutations. The resulting data was graphed using R (R Core Team & others 2013) and the ggplot package (Wickham 2016). A Tukey-Kramer test was performed using JMP ® version 15.0.0 (SAS Institute Inc., Cary, NC) to test the association between flanking markers, as well as a haplotype representing both markers simultaneously, and GSB disease severity in the population.

Synteny Analysis and Candidate Genes

The cucurbit genomics genome browser (Zheng et al. 2019) (http://cucurbitgenomics.org) was used to identify gene predictions for the *C. lanatus* 97103v2 genome (Guo et al. 2019). These genes were then examined for predicted functions related to disease resistance. The cucurbit genomics synteny browser (http://cucurbitgenomics.org) was used to check the synteny of the *Qgsb5.2* to other reported GSB resistance QTL in cucurbits.

Results

Phenotypic Data

The phenotypic distribution for the population was skewed (Shapiro-Wilk test $P = < 0.0001$) towards lower disease symptom severity (Fig. 2.1). PI 189225 (resistant parent), Sugar Baby (susceptible parent) and the F_1 had disease severity scores of 1.5, 4.6 and 1.7, respectively (Fig. 2.2). For the re-screen of the 20 most resistant and 20 most susceptible families, PI 189225, Sugar Baby and the F_1 had disease severity scores of 1.0, 4.5 and 3.9 respectively (data not shown).

QTL-seq

DNA sequences were obtained from each bulk consisting of 148,037,545 reads for the susceptible bulk and 149,620,933 reads for the resistant bulk. Alignment to the *C. lanatus* 97103_v2 genome (Guo et al. 2019) resulted in 145,179,598 mapped reads with a mapping ratio of 98.07%, with 89.53% of reads properly paired and an average coverage of 56× for the susceptible bulk, and 147,148,116 mapped reads with a mapping ratio of 98.53% with 89.79% of reads properly paired and an average coverage of 57× for the resistant bulk. 6,186,663 SNPs were identified from the aligned reads (Table 2.1). Initial filtering with GATK reduced the number of SNPs to 5,806,149. The second round of filtering using QTLseqr filtered another 5,567,799 leaving 238,350 high quality SNPs for analysis. Δ-SNP Index analysis using QTLseqr revealed four regions in which the tricube smoothed Δ-SNP Index exceeded the 95% confidence threshold, one region each on chromosomes 2, 5, 9, and 11 (Fig. 2.3, Table 2.2). The peak region on chromosome 2 exceeding the 95% confidence interval spanned 1,037,352 base pairs, from 5,835,675 bp to 6,873,027 bp, with a peak Δ-SNP index of 0.36. The peak region on chromosome 5 exceeding the confidence interval spanned 2,904,205 base pairs, from 25,465,570 bp to 28,369,775 bp, with a peak Δ-SNP Index of 0.45. The peak on chromosome 5 exceeded the 99% confidence interval. The peak region on chromosome 9 exceeding the 95% confidence interval spanned 379,167 base pairs, from 8,570,733 bp to 8,949,900 bp, with a peak Δ-SNP Index of 0.34. The peak region on chromosome 11 exceeding the 95% confidence interval spanned 503,798 base pairs, from 30,375,412 bp to 30,879,210 bp, with a peak Δ-SNP Index of -0.38.

QTL Mapping

Twenty-eight KASP marker assays were developed spanning the chromosomal regions of interest. Genetic mapping resulted in four linkage groups spanning 19.61, 61.06, 5.01, and 5.90

cM, on chromosomes 2, 5, 9, and 11, respectively (Fig 2.4). Segregation distortion was observed for several markers on the map, predominantly in the direction of the susceptible SB parent (Fig. 4.2). QTL mapping (Fig. 2.5) resulted in a single significant peak on chromosome 5, between SNP S5_25968975 (KASP assay ClGSB5.2–1) and S5_26536280 (KASP assay ClGSB5.2–2) at 14.0 cM (LOD = 3.37; PVE = 13.3%), with left and right 1-LOD confidence intervals of 11.5 cM and 16.5 cM. Additive and dominance values for this QTL were 0.5414 and 0.1116, respectively. Significant preferential segregation of the susceptible alleles was observed for seven out of the ten markers mapped on chromosome five ($\chi 2$ $P < 0.05$). To determine whether the QTL identified in the current study overlaps with *Qgsb5.1* (syn. *ClGSB5.1*) identified by Gimode et al. (2021), the marker most closely associated to *Qgsb5.1* (ClGSB5.1–1) was included in the map (Fig. 2.4). ClGSB5.1–1 mapped 44.5 cM outside the confidence interval of the current QTL and it was therefore concluded that the QTL identified in the current study represents a novel QTL (*Qgsb5.2)*. For the two KASP assays closest to *Qgsb5.2*, individuals homozygous for the allele from the susceptible parent (A/A or T/T) were significantly less resistant to GSB than individuals homozygous for the allele from the resistant parent (C/C) (Fig. 2.6). Assay ClGSB5.2–1 showed significant ($P = 0.001$) association with disease resistance (C/C = 2.1; T/T = 2.9), with an R^2 value of 12.1%. Assay ClGSB5.2–2 showed significant ($P = 0.001$) association with disease resistance (C/C = 1.6; A/A = 2.6), with an R^2 value of 12.3%. The haplotype representing both ClGSB5.2-1 and ClGSB5.2-2 showed a significant ($P = 0.014$) association with disease resistance (C/C:C/C = 1.6; T/T:A/A = 2.6) for individuals homozygous at both loci for the resistant or susceptible alleles, with and R^2 value of 12.2% (data not shown). The QTL identified by QTL-seq on chromosomes 2, 9, and 11 could not be confirmed by genetic mapping.

Synteny Analysis and Candidate Genes

The 567,305 bp region of *Qgsb5.2* contained 38 predicted genes. Three of these genes, an Ethylene-responsive transcription factor 2 gene (*Cla97C05G096890*) (Brown et al. 2003), a histidine kinase 5 gene (*Cla97C05G096980*) (Pham & Desikan 2012) and an enhanced disease resistance 2-like protein gene (*Cla97C05G097030*) (Vorwerk et al. 2007), are probable fungal disease resistance genes based on their similarity to genes known to be related to fungal resistance in *Arabidopsis thaliana* (Guo et al. 2019). No non-synonymous polymorphisms were detected in the exons of these genes within our sequencing data. The *Qgsb5.2* region was not found to be syntenic to any previously identified GSB resistance QTL in cucurbits (Lou et al. 2013, Liu et al. 2017, Zhang et al. 2017, Ren et al. 2019, Gimode et al. 2021, Lee et al. 2021).

Discussion

GSB causes significant yield losses for watermelon growers (Keinath & Duthie 1998). Efforts to control the disease using genetic resistance have recently been confounded by the discovery that the disease is caused by three *Stagonosporopsis* species (Stewart et al. 2015). A study by Gimode et al. (2019) showed significant differences in disease severity caused by different *Stagonosporopsis* isolates in different watermelon genotypes, but no significant genotype × isolate interactions were observed. Unraveling the host resistance response to different *Stagonosporopsis* species and isolates is likely key to developing cultivars with field resistance to this disease. Here we report a novel QTL from PI 189225 associated with resistance to *S. citrulli*, the most common species causing GSB in the southeastern US.

A continuous distribution was observed for disease symptom severity in the Sugar Baby × PI189225 population, indicating quantitative control of GSB resistance in this population. Additionally, both resistant and susceptible families of the population exhibited transgressive segregation relative to the parents. This contributes additional evidence to the hypothesis that GSB

resistance is quantitatively controlled (Gusmini et al. 2017). Other recent studies have reached similar conclusions (Lou et al. 2013, Gusmini et al. 2017, Liu et al. 2017, Zhang et al. 2017, Hassan et al. 2019, Ren et al. 2019, Gimode et al. 2021), in contrast to earlier reports which proposed resistance in PI 189225 was monogenic (Norton 1979, Zuniga et al. 1999, Frantz & Jahn 2004)

QTL-seq identified QTL on chromosomes 2, 5, 9, and 11, and *Qgsb5.2* was confirmed by genetic mapping. Similar results were obtained by Ramos et al. (2020) in a study mapping *Phytophthora capsici* resistance in squash. Possible explanations for the inability to confirm certain QTL, include the small population size and/or a small contribution to resistance by individual QTL (Vales et al. 2005). The unconfirmed QTL could also have been false positives.

The KASP assays (ClGSB5.2–1 & ClGSB5.2–2) linked to *Qgsb5.2* were effective at explaining 12% of the resistance observed in this population. While this shows that *Qgsb5.2* can be effectively tracked is also underlines the need for the identification of more resistance QTL, as a 12% increase in resistance would likely not lead to any appreciable reduction in fungicide use by farmers. It is interesting that no QTL explaining a larger percentage of the observed variation where detected, despite transgressive segregation being observed for disease resistance in the population. This likely indicates the resistance of PI 189225 is coming from many QTL with small effects, below the detection resolution of this study. The two markers most closely linked to *Qgsb5.2* (ClGSB5.2-1 and ClGSB5.2-2) exhibited severe segregation distortion (ClGSB5.2-1: $P < 0.0001$; ClGSB5.2-2: $P = 0.0015$) in the direction of the SB alleles. Segregation distortion was observed for all markers within 12 cM of *Qgsb5.2*. The significant segregation distortion is likely due to the interspecific nature of the cross which originated this population. Segregation distortion in *C. lanatus* × *C. amarus* crosses is a common phenomenon (Sandlin et al. 2012, Gimode et al. 2021) and complicates introgression of desirable alleles from *C. amarus* into elite watermelon.

Two previous studies using the same resistant source (PI 189225) identified two different QTL on chromosome 8 and one on chromosome 6 (Ren et al. 2019; Lee et al. 2021). A possible explanation for the different QTL identified in different studies is the use of different phenotyping methods or rating systems. The study by Lee et al. (2021) rated stem lesions and leaf lesions separately and mapped both separately, while Ren et al. (2019) rated plants based on the symptoms on four true leaves. The current study rated plants based on the symptoms of the first two true leaves. Another possible explanation for the identification of different QTL is the use of different species of the GSB-causing fungi. Ren et al. (2019) used an isolate of *S. cucurbitacearum,* while the current study was conducted using an isolate of *S. citrulli*. The specific species of *Stagonosporopsis* used by Lee et al. (2021) is not known. These three studies suggest that different loci might control resistance to different species of *Stagonosporopsis* causing GSB. Ideally, repeated studies using the same phenotyping conditions and rating systems should be conducted under field conditions, where evidence is emerging that populations of multiple species of *Stagonosporopsis* can exist within a single field (Li & Brewer 2016).

Qgsb5.2 is at a different location than the QTL identified by Gimode et al. (2021) using the same *S. citrulli* isolate (12178A), but a different resistant parent (PI 482276). This seems to indicate that the two PIs contain distinct resistance loci. This could be beneficial to breeders as it would allow their effects to be combined through gene pyramiding.

Of the 38 predicted genes within the *Qgsb5.2* region there are three genes of particular interest for their potential association with disease resistance. *Cla97C05G096980* is homologous to the histidine kinase 5 gene of *Arabidopsis thaliana,* which has been shown to regulate the production of reactive oxygen species in response to stressors including necrotrophic fungi (Pham et al. 2012). *Cla97C05G097030* is similar to the *enhanced disease resistance 2* gene in *A. thaliana*

which has been shown to negatively regulate salicylic acid-based defenses and cell death in powdery mildew infections (Vorwerk et al. 2007). *Cla97C05G096890* is homologous to the *Ethylene-responsive transcription factor 2* gene from *A. thaliana*, which has been shown to be related to signaling pathways involved in resistance to *Alternaria brassicicola* (McGrath et al. 2005). Interestingly, salicylic acid-based signaling tends to be related to defense against biotrophic disease such as powdery mildew, while ethylene based signaling tends to be related to defense against necrotrophic diseases like those caused by *A. brassicicola* (Spoel et al. 2007). Given that GSB causing *Stagonosporopsis* species are thought to feed necrotrophically, *Cla97C05G096980* and *Cla97C05G096890* are likely candidate genes for this QTL. A study examining the effects of knocking out each gene and the effects that has on resistance could shed light on this question.

The identification of *Qgsb5.2* brings the total number of QTL identified for GSB resistance to five. However, it remains unclear if these QTL contribute resistance to all GSB causing *Stagonosporopsis* species and isolates. More research is needed to determine the utility of these QTL against different species and isolates of *Stagonosporopsis* under field conditions. However, in light of the discovery of distinct QTL by this study, Ren et al. (2019), and Lee et al. (2021) in germplasm derived from the same resistant PI, it is beginning to appear as if field level GSB resistance will require the incorporation of a number of different QTL. Pyramiding multiple resistance genes can allow breeders to develop plants that are resistant to many different isolates or species of disease-causing pathogens, while increasing the durability of resistance to individual pathogen isolates, as shown for wheat stem rust (Zhang et al. 2019). QTL mapping resistance to multiple isolates of GSB-causing fungi in the same study would contribute greatly to our understanding of this issue and may provide the requisite QTL for pyramiding. The QTL identified

in this study represents one part of that potential resistance gene pyramid to reduce the need to spray fungicides in order to control the disease.

Acknowledgements

This research was partially funded by the National Institute of Food and Agriculture, U.S. Department of Agriculture, award numbers 2015-51181-24285 and 2020-51181-32139.

References

Andrews, S. 2010. FastQC: a quality control tool for high throughput sequence data. Babraham Bioinformatics, Babraham Institute, Cambridge, United Kingdom.

Boyhan, G., J. Norton and B. Abrahams. 1994. Screening for resistance to anthracnose (race 2), gummy stem blight, and root knot nematode in watermelon germplasm. Cucurbit Genet. Coop. Rep. 17:106–110.

Branham, S.E., W. Patrick Wechter, S. Lambel, L. Massey, M. Ma, J. Fauve, M.W. Farnham and A. Levi. 2018. QTL-seq and marker development for resistance to Fusarium oxysporum f. sp. niveum race 1 in cultivated watermelon. Mol. Breed. 38:139.

Brown, R.L., K. Kazan, K.C. McGrath, D.J. Maclean and J.M. Manners. 2003. A role for the GCC-box in jasmonate-mediated activation of the PDF1.2 gene of Arabidopsis. Plant Physiol. 132:1020–1032.

Clevenger, J., Y. Chu, C. Chavarro, S. Botton, A. Culbreath, T.G. Isleib, C.C. Holbrook and P. Ozias-Akins. 2018. Mapping late leaf spot resistance in peanut (*Arachis hypogaea*) using QTL-seq reveals markers for marker-assisted selection. Front. Plant Sci. 9.

Danecek, P., A. Auton, G. Abecasis, C.A. Albers, E. Banks, M.A. DePristo, R.E. Handsaker, G. Lunter, G.T. Marth, S.T. Sherry, G. McVean and R. Durbin. 2011. The variant call format and VCFtools. Bioinformatics 27:2156–2158.

Fall, L.A., J. Clevenger and C. McGregor. 2018. Assay development and marker validation for marker assisted selection of *Fusarium oxysporum* f. sp. *niveum* race 1 in watermelon. Mol. Breed. 38:130.

Frantz, J.D. and M.M. Jahn. 2004. Five independent loci each control monogenic resistance to gummy stem blight in melon (Cucumis melo L.). Theor. Appl. Genet. 108:1033–1038.

Gimode, W., K. Bao, Z. Fei and C. McGregor. 2021. QTL associated with gummy stem blight resistance in watermelon. Theor. Appl. Genet. 134:573–584.

Gimode, W., M. Lonnee and C. McGregor. 2019. Resistance response of *Citrullus* genotypes to *Stagonosporopsis* spp. isolates causing gummy stem blight. Cucurbit Genet. Coop. Rep. 42:1–6.

Guo, S., S. Zhao, H. Sun, X. Wang, S. Wu, T. Lin, Y. Ren, L. Gao, Y. Deng, J. Zhang, X. Lu, H. Zhang, J. Shang, G. Gong, C. Wen, N. He, S. Tian, M. Li, J. Liu, Y. Wang, Y. Zhu, R. Jarret, A. Levi, X. Zhang, S. Huang, Z. Fei, W. Liu and Y. Xu. 2019. Resequencing of 414 cultivated and wild watermelon accessions identifies selection for fruit quality traits. Nat. Genet. 51:1616–1623.

Gusmini, G., L.A. Rivera-Burgos and T.C. Wehner. 2017. Inheritance of resistance to gummy stem blight in watermelon. HortScience 52:1477–1482.

Gusmini, G., R. Song and T.C. Wehner. 2005. New sources of resistance to gummy stem blight in watermelon. Crop Sci. 45:582–588.

Hassan, M.Z., M.A. Rahim, H.-J. Jung, J.-I. Park, H.-T. Kim and I.-S. Nou. 2019. Genome-wide characterization of NBS-encoding genes in watermelon and their potential association with gummy stem blight resistance. Int. J. Mol. Sci. 20:902.

Keinath, A.P. 2011. From native plants in central Europe to cultivated crops worldwide: the emergence of *Didymella bryoniae* as a cucurbit pathogen. HortScience 46:532–535.

Keinath, A.P. and J.A. Duthie. 1998. Yield and quality reductions in watermelon due to anthracnose, gummy stem blight, and black rot. Recent Res. Dev. Plant Pathol. 77–90.

Lee, E.S., D.-S. Kim, S.G. Kim, Y.-C. Huh, C.-G. Back, Y.-R. Lee, M.I. Siddique, K. Han, H.-E. Lee and J. Lee. 2021. QTL mapping for gummy stem blight resistance in watermelon (*Citrullus* spp.). Plants 10:500.

Li, H. 2013. Aligning sequence reads, clone sequences and assembly contigs with BWA-MEM. ArXiv Prepr. ArXiv13033997.

Li, H., B. Handsaker, A. Wysoker, T. Fennell, J. Ruan, N. Homer, G. Marth, G. Abecasis, R. Durbin, and 1000 Genome Project Data Processing Subgroup. 2009. The Sequence Alignment/Map format and SAMtools. Bioinforma. Oxf. Engl. 25:2078–2079.

Li, H.-X. and M.T. Brewer. 2016. Spatial genetic structure and population dynamics of gummy stem blight fungi within and among watermelon fields in the southeastern United States. Phytopathology 106:900–908.

Liu, S., Y. Shi, H. Miao, M. Wang, B. Li, X. Gu and S. Zhang. 2017. Genetic analysis and QTL mapping of resistance to gummy stem blight in *Cucumis sativus* seedling stage. Plant Dis. 101:1145–1152.

Lou, L., H. Wang, C. Qian, J. Liu, Y. Bai and J. Chen. 2013. Genetic mapping of gummy stem blight (*Didymella bryoniae*) resistance genes in Cucumis sativus-hystrix introgression lines. Euphytica 192:359–369.

Mansfeld, B.N. and R. Grumet. 2018. QTLseqr: an R package for bulk segregant analysis with next-generation sequencing. Plant Genome 11.

McGrath, K.C., B. Dombrecht, J.M. Manners, P.M. Schenk, C.I. Edgar, D.J. Maclean, W.-R. Scheible, M.K. Udvardi and K. Kazan. 2005. Repressor- and activator-type ethylene response factors functioning in jasmonate signaling and disease resistance identified via a

genome-wide screen of *Arabidopsis* transcription factor gene expression. Plant Physiol. 139:949–959.

McKenna, A., M. Hanna, E. Banks, A. Sivachenko, K. Cibulskis, A. Kernytsky, K. Garimella, D. Altshuler, S. Gabriel, M. Daly and M.A. DePristo. 2010. The Genome Analysis Toolkit: a MapReduce framework for analyzing next-generation DNA sequencing data. Genome Res. 20:1297–1303.

Meng, L., H. Li, L. Zhang and J. Wang. 2015. QTL IciMapping: Integrated software for genetic linkage map construction and quantitative trait locus mapping in biparental populations. Crop J., Special Issue: Breeding to Optimize Agriculture in a Changing World 3:269–283.

Michelmore, R.W., I. Paran and R.V. Kesseli. 1991. Identification of markers linked to disease-resistance genes by bulked segregant analysis: a rapid method to detect markers in specific genomic regions by using segregating populations. Proc. Natl. Acad. Sci. 88:9828–9832.

Norton, J.D. 1979. Inheritance of resistance to gummy stem blight [caused by *Didymella bryoniae*] in watermelon. HortScience USA 14:630–632.

Norton, J.D., G.E. Boyhan, D.A. Smith and B.R. Abrahams. 1993. "AU-Golden Producer" watermelon. HortScience 26:681–682.

Norton, J.D., G.E. Boyhan, D.A. Smith and B.R. Abrahams. 1995. "AU-Sweet Scarlet" watermelon. HortScience 30:393–394.

Norton, J.D., R.D. Cosper, D.A. Smith and K.S. Rymal. 1986. "AU-Jubilant" and "AU-Producer" watermelons. HortScience USA 21:1460–1461.

Pham, J. and R. Desikan. 2012. Modulation of ROS production and hormone levels by AHK5 during abiotic and biotic stress signaling. Plant Signal. Behav. 7:893–897.

Pham, J., J. Liu, M.H. Bennett, J.W. Mansfield and R. Desikan. 2012. Arabidopsis histidine kinase 5 regulates salt sensitivity and resistance against bacterial and fungal infection. New Phytol. 194:168–180.

Quinlan, A.R. and I.M. Hall. 2010. BEDTools: a flexible suite of utilities for comparing genomic features. Bioinformatics 26:841–842.

R Core Team, Rf. and others. 2013. R: A language and environment for statistical computing. R foundation for statistical computing Vienna, Austria.

Ramos, A., Y. Fu, V. Michael and G. Meru. 2020. QTL-seq for identification of loci associated with resistance to Phytophthora crown rot in squash. Sci. Rep. 10:5326.

Ren, R., J. Xu, M. Zhang, G. Liu, X. Yao, L. Zhu and Q. Hou. 2019. Identification and molecular mapping of a gummy stem blight resistance gene in wild watermelon (*Citrullus amarus*) germplasm PI 189225. Plant Dis. 104:16–24.

Schwartz, H.F. and D.H. Gent. 2007. Gummy stem blight and black rot (cucumber, melon, pumpkin, squash, and zucchini). *In* High Plains IPM Guide. Cooperative effort of the University of Wyoming, University of Nebraska, Colorado State University and Montana State University.

Song, R., G. Gusmini and T.C. Wehner. 2004. Screening the watermelon germplasm collection for resistance to gummy stem blight. XXVI Int. Hortic. Congr. Adv. Veg. Breeding Acta Hortic. 63–68.

Species Fungorum. Entry for Stagonosporopsis cucurbitacearum. 9 Sept. 2020. <http://www.speciesfungorum.org/GSD/GSDspecies.asp?RecordID=515660>

Spoel, S.H., J.S. Johnson and X. Dong. 2007. Regulation of tradeoffs between plant defenses against pathogens with different lifestyles. Proc. Natl. Acad. Sci. U. S. A. 104:18842–18847.

Stewart, J.E., A.N. Turner and M.T. Brewer. 2015. Evolutionary history and variation in host range of three *Stagonosporopsis* species causing gummy stem blight of cucurbits. Fungal Biol. 119:370–382.

Sumner, D. and M. Hall. 1993. Resistance of watermelon cultivars to Fusarium wilt and gummy stem blight. Biol. Cult. Tests 8:36.

Takagi, H., A. Abe, K. Yoshida, S. Kosugi, S. Natsume, C. Mitsuoka, A. Uemura, H. Utsushi, M. Tamiru, S. Takuno, H. Innan, L.M. Cano, S. Kamoun and R. Terauchi. 2013. Qtl-seq: rapid mapping of quantitative trait loci in rice by whole genome resequencing of DNA from two bulked populations. Plant J. 74:174–183.

Vales, M., C. Schön, F. Capettini, X. Chen, A. Corey, D. Mather, C. Mundt, K. Richardson, J. Sandoval-Islas, H. Utz, and others. 2005. Effect of population size on the estimation of QTL: a test using resistance to barley stripe rust. Theor. Appl. Genet. 111:1260–1270.

Voorrips, R.E. 2002. MapChart: Software for the graphical presentation of linkage maps and QTLs. J. Hered. 93:77–78.

Vorwerk, S., C. Schiff, M. Santamaria, S. Koh, M. Nishimura, J. Vogel, C. Somerville and S. Somerville. 2007. EDR2 negatively regulates salicylic acid-based defenses and cell death during powdery mildew infections of *Arabidopsis thaliana*. BMC Plant Biol. 7:35.

Wickham, H. 2016. ggplot2: elegant graphics for data analysis. Springer-Verlag New York.

Wightwick, A., R. Walters, G. Allinson, S. Reichman and N. Menzies. 2010. Environmental risks of fungicides used in horticultural production systems. Fungicides 1:273–304.

Zhang, B., D. Chi, C. Hiebert, T. Fetch, B. McCallum, A. Xue, W. Cao, R. Depauw and G. Fedak. 2019. Pyramiding stem rust resistance genes to race TTKSK (Ug99) in wheat. Can. J. Plant Pathol. 41:443–449.

Zhang, S., S. Liu, H. Miao, Y. Shi, M. Wang, Y. Wang, B. Li and X. Gu. 2017. Inheritance and QTL mapping of resistance to gummy stem blight in cucumber stem. Mol. Breed. 37:49.

Zheng, Y., S. Wu, Y. Bai, H. Sun, C. Jiao, S. Guo, K. Zhao, J. Blanca, Z. Zhang, S. Huang, Y. Xu, Y. Weng, M. Mazourek, U. K. Reddy, K. Ando, J.D. McCreight, A.A. Schaffer, J. Burger, Y. Tadmor, N. Katzir, X. Tang, Y. Liu, J.J. Giovannoni, K.-S. Ling, W.P. Wechter, A. Levi, J. Garcia-Mas, R. Grumet and Z. Fei. 2019. Cucurbit Genomics Database (CuGenDB): a central portal for comparative and functional genomics of cucurbit crops. Nucleic Acids Res. 47:D1128–D1136.

Zuniga, T.L., J.P. Jantz, T.A. Zitter and M.K. Jahn. 1999. Monogenic dominant resistance to gummy stem blight in two melon (*Cucumis melo*) accessions. Plant Dis. 83:1105–1107.

Table 2.1: Mapping statistics for short reads generated by sequencing of the resistant and susceptible DNA bulks.

Sample	Total Reads	Mapped Reads	Mapping Ratio (%)	Properly Paired (%)	Average Coverage (x)
Susceptible Bulk	148,037,545	145,179,598	98.07%	89.53%	56
Resistant Bulk	149,620,933	147,148,116	98.35%	89.79%	57

Table 2.2: Quantitative trait loci identified for gummy stem blight resistance by comparing the susceptible and resistant bulks of the Sugar Baby × PI 189223 $F_{2:3}$ population. Locations are based on the *C. lanatus* 91703_v2 genome sequence (Guo et al. 2019).

Chr.	Start (bp)	End (bp)	Length (bp)	Total # of SNPs	Peak Δ-SNP Index	Peak Δ-SNP Index Position
2	5,835,675	6,873,027	1,037,352	482	0.36	6,517,652
5	25,465,570	28,369,775	2,904,205	1677	0.45	26,916,783
9	8,570,733	8,949,900	379,167	174	0.34	8,843,908
11	30,375,412	30,879,210	503,798	147	-0.38	30,879,210

Table 2.3: KASP assays for flanking SNPs for GSB resistance QTL on chromosome 5 (*Qgsb5.2*).

KASP Assay	Ta (°C)	SNP	Primer type	Primer sequence (5′-3′)	Allele
ClGSB5.2–2	57	UGA5_26536280	FAM	GAAGGTCGGAGTCAACGGATTCCT ACTTTCCATGCACATGCTCTC	SB (S)
			VIC	GAAGGTGACCAAGTTCATGCTCCTA CTTTCCATGCACATGCTCTA	PI 189225 (R)
			Reverse	CCGGGTAACTGTCCAGATCG	
ClGSB5.2–1	57	UGA5_25968975	FAM	GAAGGTGACCAAGTTCATGCT CCATTGGAATTGCCACTAGTTTGC	SB
			VIC	GAAGGTCGGAGTCAACGGATTCCA TTGGAATTGCCACTAGTTTGT	PI 189225
			Reverse	TCAAAGGTCTGCTGGCTCCT	

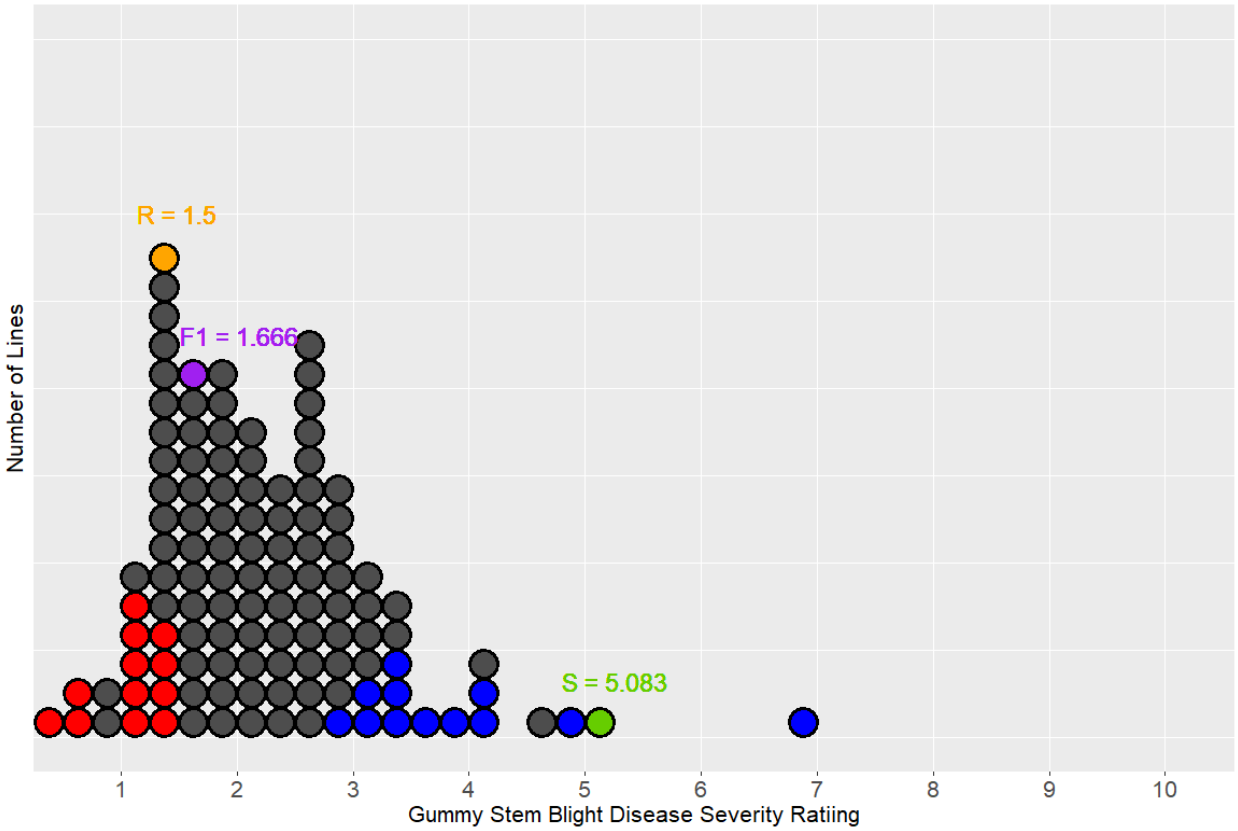

Figure 2.1: Stacked dot plots showing the distribution of the average disease severity of the $F_{2:3}$ families (n = 111) of a cross between Sugar Baby (S) and PI 189225 (R). Red and blue dots represent the families selected to generate the resistant and susceptible DNA bulks, respectively. The orange, purple, and green dots represent the average phenotypic values for PI 189225, the F_1, and Sugar Baby, respectively.

Figure 2.2: Gummy stem blight disease severity in PI 189225 (resistant), the $F_{1,}$ and Sugar Baby (susceptible) after infection with *S. citrulli*.

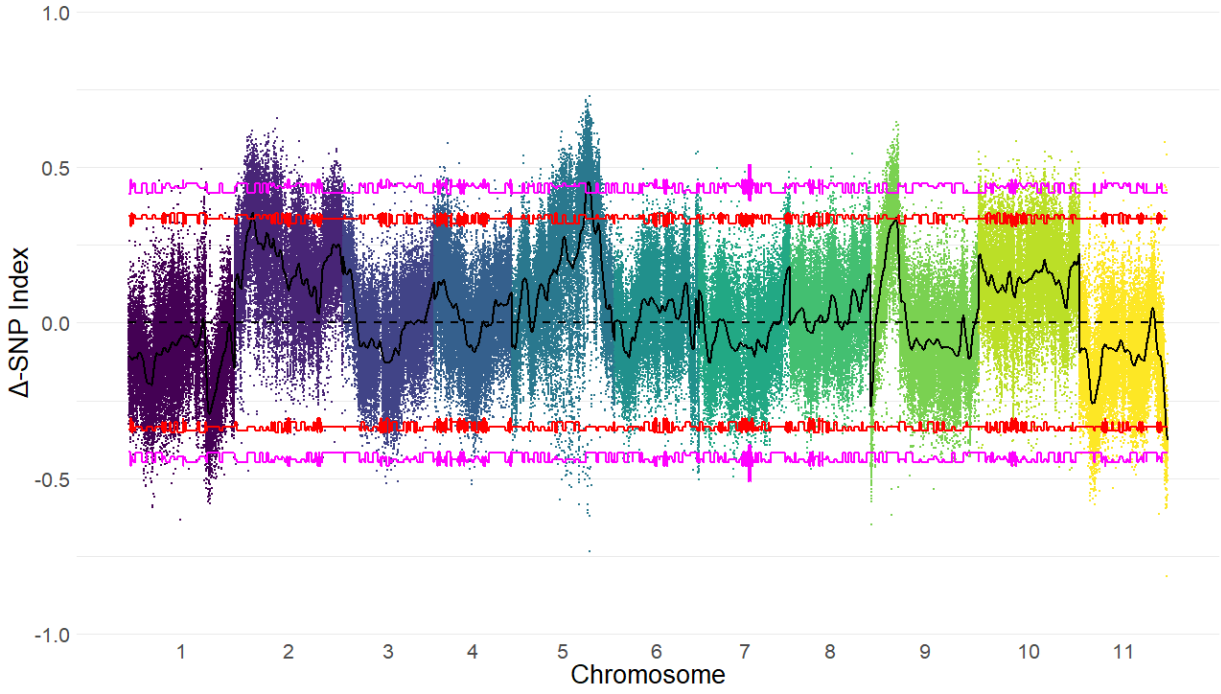

Figure 2.3: The Δ-SNP index of each identified SNP generated from the gummy stem blight resistant and susceptible bulks. Individual colored points represent individual SNPs, with each color representing a different chromosome. The black line represents the tricube smoothed Δ-SNP index value using a 1Mb sliding window. The red line represents the 95% confidence interval and the pink line represent the 99% confidence interval. A positive Δ-SNP index represents SNPs differing from the reference genome which are potentially contributing to the trait of interest, while regions with a negative Δ-SNP index represent SNPs shared with the reference genome which are potentially contributing to the trait of interest. Regions where the black line exits the bounds of the confidence intervals represent potential QTL for gummy stem blight resistance. Δ-SNP indices were calculated using QTLseqr (Mansfeld & Grumet 2018).

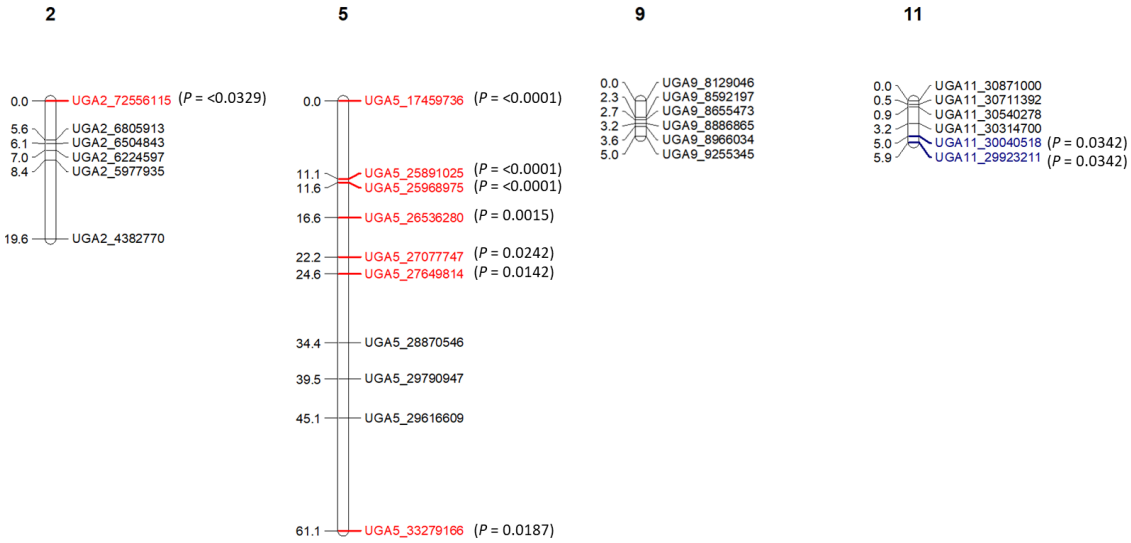

Figure 2.4: Linkage maps of the regions on chromosomes 2, 5, 9, and 11 identified by QTLseq. These maps are comprised of 6, 10, 6 and 6 markers respectively with lengths of 19.6, 61.1 5.0 and 5.9 cM. Markers indicated in red are preferentially segregating for the alleles contributed by SB, and markers indicated in blue are preferentially segregating for the alleles contributed by PI 189225. *P* values for Chi^2 goodness of fit test are given next to each marker.

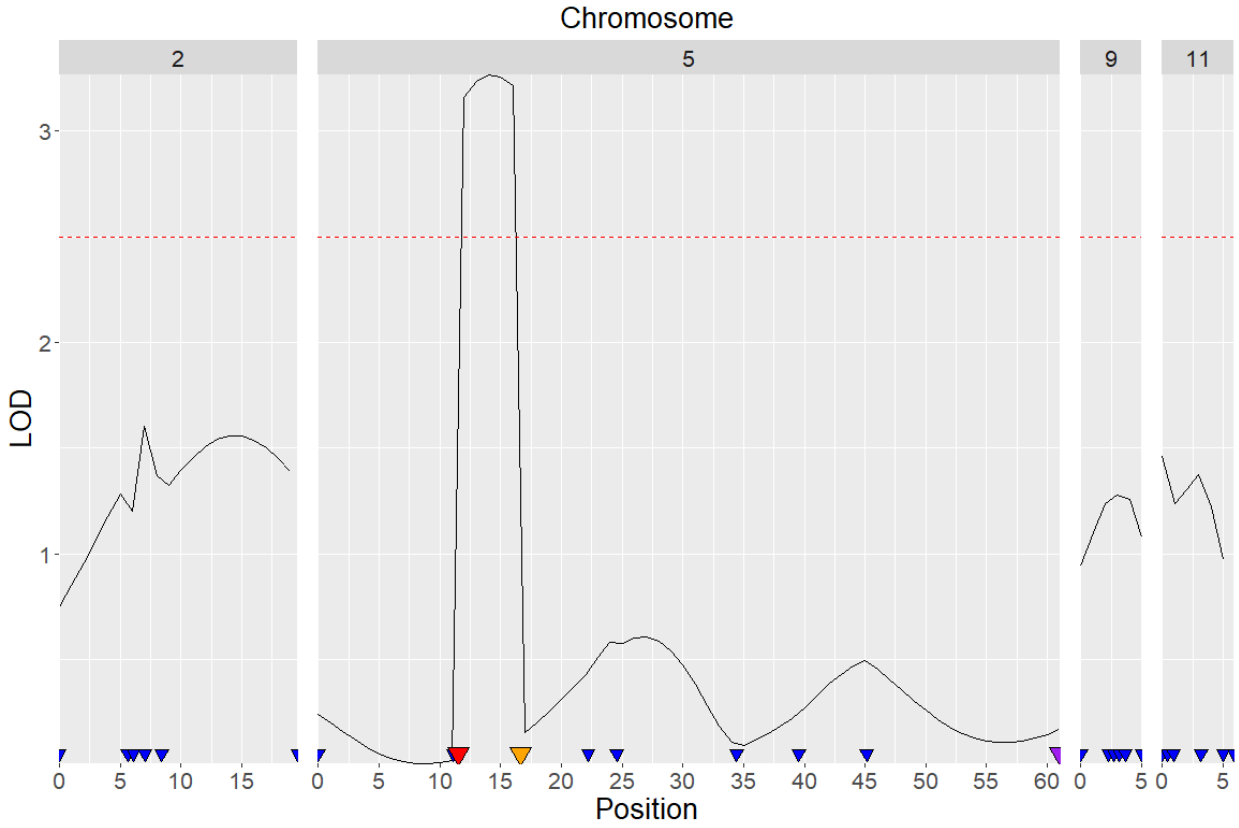

Figure 2.5: QTL associated with Gummy stem blight resistance in the Sugar Baby × PI 189225 $F_{2:3}$ population (n = 111). The red dashed line indicates the LOD threshold (1,000 permutations), while the triangles indicate the position of the KASP markers. The purple triangle represents marker ClGSB5.1–1, which was linked to *Qgsb5.1* in the Gimode et al. (2021) study. The red triangle represents marker ClGSB5.2-1, and the orange triangle represents marker ClGSB5.2-2, both of which are linked to *Qgsb5.2*. All other markers are represented by blue triangles.

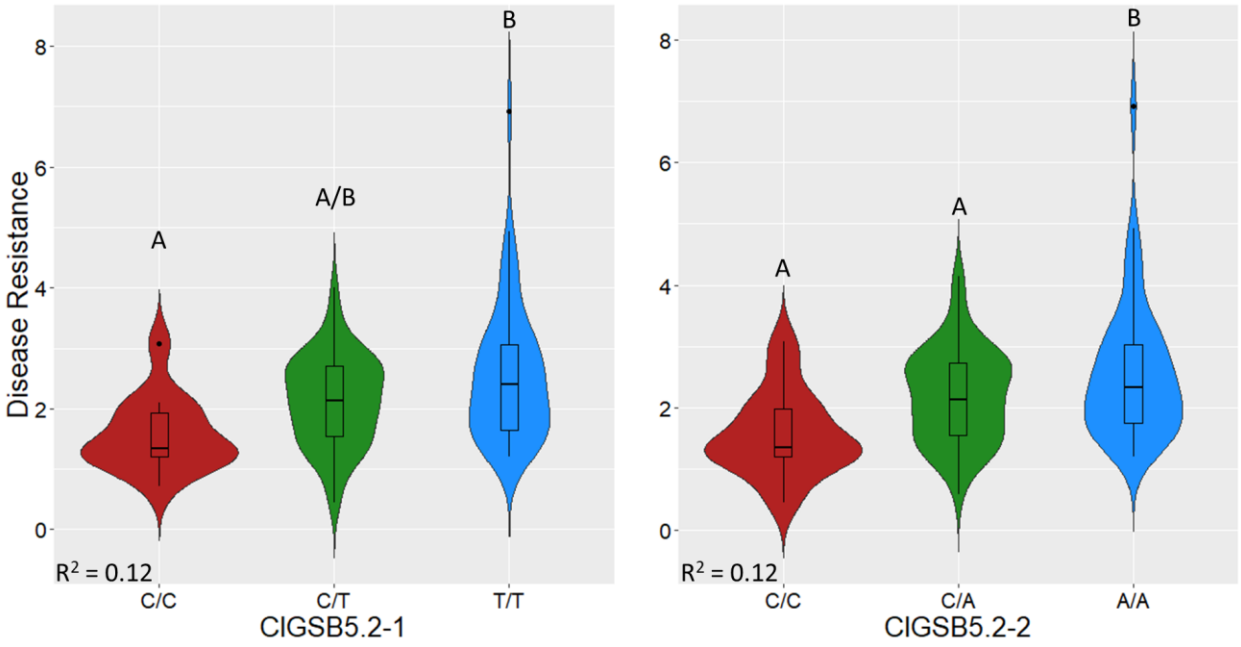

Figure 2.6: Violin plots showing the association of ClGSB5.2-2 and ClGSB5.2-2 genotypes with disease severity in the Sugar Baby × PI 189225 population (n=111). In both KASP assays, the C/C genotype represent individuals that are homozygous for the allele from the resistant parent (PI 189225). Box and whisker plots show median and quartile ranges of each group. Different letters above the plots indicate significant differences based on a Tukey-Kramer test.

CHAPTER 3

QTL CONTROLING RIND THICKNESS IN WATERMELON

[1]Adams, L., Josiah, S., Legendre, R., McGregor, C. To be submitted.

Abstract

Rind thickness is an important trait in watermelon (*Citrullus lanatus*) governing its ability to be shipped to global markets. This desire for a thick, shippable rind must be balanced against consumer preference for a rind which makes up a small portion of the fruit. Understanding the mechanism controlling rind thickness (RTH) would be useful to watermelon breeders to balance these contrasting requirements. In this study we used three populations to examine the effects of three QTL (*QFD2.2, QFSI3.1,* and *QRTH5.1)* on fruit diameter (FD), RTH, and RTH as a proportion of fruit diameter (RRP). *QFD2.2* was associated with FD, RTH and RRP in two of the populations. *QRTH5.1* was confirmed as a QTL associated with RTH in one population and an interaction was observed between *QFD2.2* and *QRTH5.1*. In the same population, *QFSI5.1* was associated with FD and RRP and an interaction between *QFSI5.1* with *QFD2.2* was observed for RRP. Our results indicate that major fruit size QTL are associated with RTH in diverse backgrounds. *QRTH5.1* is not colocalized with any known fruit size QTL, but significant interactions were observed between this locus and fruit size loci. The marker assays developed in this study for *QFD2.2* and *QRTH5.1* should be useful in future studies and selection of these loci in watermelon breeding programs.

Keywords: Watermelon, *Citrullus lanatus*, Rind Thickness, Fruit Diameter, Rind Ratio Percentage, QTLseq, QTL Mapping

Introduction

Watermelon (*Citrullus lanatus*) is an important horticultural crop, with over 100 million tonnes grown around the world in 2019. Sixty percent of the world watermelon crop is grown in China, but it is an economically important crop in many other countries around the world, including the United States of America. US watermelon growers produced nearly 1.7 million tonnes of watermelon from a planting of over 41 thousand hectares in 2019 (FAOSTAT 2020).

For much of history, watermelons were sold locally during a short production window. However, improvements in packaging and shipping technologies now allow growers to service much wider markets, and consumers to purchase watermelon shipped from long distances when it is not locally in season (Perkins-Veazie et al. 2012). This global market has led to a need for highly durable fruit which are able to withstand the rigors of shipping, as damage during shipping translates directly into loss of revenue for the industry (Breakiron 1954). To meet this demand, growers have turned to cultivars with thicker rinds, which have been shown to be more resistant to cracking (Sadrnia et al. 2009). Rind toughness has been shown to influence durability independently of RTH, with tough rind (*E)* being dominant over explosive rind (*e)* (Porter 1937, Poole 1944). Fruit with the explosive rind trait are prone to cracking and are, therefore, unsuitable for shipping. While tough rinds are useful for shipping, explosive rind can also be a beneficial trait, allowing the unharvested fruit of a pollenizer to be easily crushed (Wehner 2012). The desire for durable rind must be balanced against consumer preferences, which dictate that the rind must account for a relatively small portion of the entire fruit (Wehner 2008). A more complete understanding of the genetic basis of RTH could allow breeders to design watermelon with precisely the correct RTH for their size to satisfy the demands of both shippers and consumers.

Previous studies have shown significant correlations between RTH and fruit size traits [fruit weight (FWT), length (FL), and width (FD)] (Sandlin et al. 2012, Yang et al. 2021). However, despite these findings small fruit with thick rind and large fruit with thin rind are observed. Sandlin et al. (2012) identified one major (*QRTH2.1*; phenotypic variation explained (PVE) = 29.3%) and one minor (*QRTH5.1;* PVE = 6.4%) QTL for RTH on chromosome two and five, respectively in the Klondike Black Seeded (KBS; *C. lanatus*) × New Hampshire Midget (NHM; *C. lanatus*) (KxN) population. *QRTH2.1* colocalized with a QTL associated with FD (*QFD2.2*; PVE = 50%), FWT (PVE = 45.7%) and FL (PVE = 10.4%). *QRTH5.1* was not colocalized with any known fruit size or shape QTL. However, *QRTH5.1* was not detected at the second experimental location (Woodlands, CA), possibly because data was only collected for a single fruit per line at this location. Yang et al. (2021) identified a QTL controlling RTH (PVE = 14.7%) in the same location as *QRTH2.1* (*QFD2.2*) using a population derived from 1061 (*C. lanatus*) × 812 (*C. lanatus*).

RTH was also found to be correlated with FL in three distinct genetic backgrounds (Sandlin et al. 2012). A QTL associated with FL (PVE = 31%) and fruit shape index (FSI; *QFSI3.1*; PVE = 21.5%) was identified by Sandlin et al. (2012) on Chromosome 3. This QTL was later mapped in different genetic backgrounds and *Cla011257*, a homolog (*ClSUN25-26-27a*) of the *SUN* gene in tomato, was proposed as a candidate gene (Kim et al. 2015; Pan et al. 2020). Previous research showed that *SUN* increases the length of the fruit along the proximal-distal axis by increasing cell numbers in tomato (Wu et al. 2011). A 159-bp deletion and a SNP in *Cla011257* were shown to be responsible for variation in FL and FSI in diverse watermelon germplasm (Dou et al. 2018; Legendre et al. 2020). KASP assays (ClSUN-1 and ClSUN-2) were designed to differentiate the three different alleles (WT, DEL, and KBS) of *ClSUN25-26-27a* (Legendre et al. 2020, Pan et al.

2020). WT represents the wild type allele and is associated with round fruit, while the DEL allele has the 159-bp deletion associated with the elongated fruit phenotype seen in cultivars such as Charleston Gray (Dou et al. 2018; (Dou et al. 2018; Legendre et al. 2020), and the KBS allele has a G to A point mutation associated with the intermediary phenotype of Klondike Black Seeded (Legendre et al. 2020). *ClSUN25-26-27a* is the likely source of the historical *O* gene (Weetman 1937, Tanaka 1957, Pan et al. 2020).

The goals of this study were to confirm the association of *QRTH5.1* with RTH and to determine the role of known fruit size and shape QTL (*QFD2.2* and *QFSI3.1*) on (i) RTH and (ii) RRP in watermelon.

Materials and Methods

Plant Material and Phenotyping

The KxN (Fig. 3.1) recombinant inbred line (RIL) population developed by Sandlin et al. (2012) was used for this study. In addition to the data collected in 2010 in Georgia and reported in Sandlin et al. (2012) (KxN2010, n=147), the population was phenotyped again in summer 2016 (KxN2016, n=147) using a randomized complete block design with one plant per replication and five replications at the Durham Horticulture Farm in Watkinsville, GA (Fall et al. 2019). One mature fruit was harvested from each plant and FD and RTH were measured as described in Sandlin et al. (2012). RRP was calculated as $\frac{RTH}{FD}\ x\ 100$. LSMeans were calculated for each trait using JMP ® version 15.0.0 (SAS Institute Inc., Cary, NC).

Two additional F_2 populations were generated from crosses between NHM and Calhoun Gray (CALG) (NHMxCALG, n=86) (Legendre et al. 2020) (Fig. 3.1), as well as Sunsugar (SS) and Sugar Baby (SB) (SSxSB, n=66) (Fig. 3.1). The NHMxCALG and SSxSB F_2 populations, as well as the parental cultivars were grown at the Horticulture Farm in Watkinsville, GA in summer

2018. Leaf material was collected from each plant and stored at -80°C. A single fruit was collected per plant, cut in half along its vertical axis and digital images of each fruit were taken as described by Legendre et al. (2020). FIJI (Schindelin et al. 2012) was used to measure FD and RTH from the raw images. FD was measured as the distance between the edges of the fruit at its widest point, while RTH was measured by taking the average of the measurement from the edge of the fruit to the start of the red flesh on each side of the fruit along the same axis as the FD measurement. The measurements were then converted from raw pixels to millimeters using measurements taken of the ruler included in each of the images. RRP was calculated as described above.

DNA Extractions, QTL Mapping and Genotyping

DNA of all plants was extracted using a modified SDS-NaCl DNA extraction method (King et al., 2017) as described by Gimode et al (2019). For a small number of samples, extractions were done using the E.Z.N.A. HP Plant DNA Mini Kit (Omega Bio-Tek Inc., Norcross, GA) due to non-amplification of some of the samples extracted using the SDS-NaCl method. DNA was quantified with an Infinite M200 Pro plate reader (Tecan Group Ltd., Mannedorf, Switzerland) using the i-control software (Tecan Group Ltd.,) and a NanoQuant PlateTM (Tecan Group Ltd.,). Samples extracted using the SDS-NaCl method were diluted to 5x, while samples extracted using the E.Z.N.A. Kits were diluted to 10 ng/µl.

A KASP assay (ClFD2.2-1) was developed for the NW0249226 SNP, the closest SNP to *QFD2.2* on the Sandlin et al. (2012) genetic map. Two KASP assays (ClRTH5.1-1 and ClRTH5.1-2) flanking *QRTH5.1* were designed by mining SNPs from QTLseq data generated in the Gimode et al. (2019) study using the same KxN population. Primer3 Plus was used for all KASP primer design (Untergasser et al. 2007). KASP PCR reactions contained 1.94 µL of 2 × KASP Master Mix (LGC Genomics LLC), 0.06 µL of KASP Primer Mix, and 2 µL of DNA (10-20 ng/µl) in a

total volume of 4 µL. The KASP Primer Mix contained 12 µL of each forward primer (100 µM), 30 µL of reverse primer (100 µM), and 46 µL of sterile distilled water. The following PCR conditions were used: 95°C for 15 minutes followed by 10 touchdown cycles of 95°C for 20 seconds, Ta+9°C (Table 3.1) for 25 seconds, and 72°C for 15 seconds, followed by 35 cycles of 95°C for 10 seconds, Ta °C (Table 3.1) for 60 seconds and 72°C for 15 seconds. KASP fluorescent end readings were measured using an Infinite M200 Pro (Tecan Group Ltd.) plate reader using the Magellan (Tecan Group Ltd.) software. Genotypes were called using KlusterCaller™ (LGC Genomics LLC).

Markers ClRTH5.1-1 and ClRTH5.1-2 were added to the KxN genetic map (Sandlin et al. 2012) using JoinMap4 (Van Ooijen 2006) and QTL mapping of FD, RTH, and RRP was conducted with ICIMapping (Meng et al. 2015). The ICIM-ADD mapping method was used with deletion of missing phenotypes, a 1 cM step, and a value of 0.001 for the probability in stepwise regression. 1000 permutations were run to determine the LOD threshold. Resulting data was graphed in R (R Core Team & others 2013) using the ggplot2 (Wickham 2016) package.

The NHMxCALG and SSxSB populations were genotyped with ClRTH5.1-1 and ClRTH5.1-2 markers for *QRTH5*.1, as well as ClFD2.2-1. Genotypic data for *ClSUN25-26-27a* (*QFSI3.1*) for the NHMxCALG and KxN populations was obtained from Legendre et al. (2020) using ClSUN-1 and ClSUN-2 marker assays, respectively, and genotypic data for this locus was obtained for the SSxSB population using ClSUN-1 and the methodology described by the same authors. The KxN population is segregating for the WT (NHM) and KBS alleles, while the NHMxCALG and SSxSB populations are segregating for the WT (NHM and SB) and DEL (CALG and SS) alleles.

Data Analysis

The following analyses were conducted with JMP ® version 15.0.0 (SAS Institute Inc., Cary, NC): Pearson correlations between FD, RTH, and RRP were calculated for KxN2010-GA and KxN2016. Pearson correlations between FD, RTH, and RRP were calculated for NHMxCALG and SSxSB. Tukey-Kramer tests were performed to test the associations among ClFD2.2-1, ClSUN-1 or 2, ClRTH5.1-1, and ClRTH5.1-2 and FD, RTH and RRP in KxN2010-GA, KxN2016, NHMxCALG, and SSxSB. Tukey-Kramer tests were performed for combinations of two of the above listed assays, and the above listed traits in order to look for interactions among the loci. Violin plots showing marker trait associations and correlation plots were made in R (R Core Team & others 2013) using the ggplot (Wickham 2016) package.

Results

Phenotypic Data

KxN2016 exhibited an approximately normal distribution for FD (Shapiro-Wilk *P* = 0.0276, Mean = 163.27, Std Dev = 28.76, KBS = 198.9, NHM = 120, F_1 = 177.3), a positively skewed distribution for RTH (Shapiro-Wilk *P* = 0.0024, Mean = 9.53, Std Dev = 3.2, KBS=10.2, NHM=4.2, F_1 = 8), and an approximately normal distribution for RRP (Shapiro-Wilk *P* = 0.292, Mean = 5.7, Std Dev = 1.4, KBS = 5.2, NHM = 3.7, F_1 = 4.5) (Fig. 3.2b, c, and d). RRP was calculated using previous data from Sandlin et al. (2012) for KxN2010 and exhibited an approximately normal distribution for RRP (Shapiro-Wilk *P* = 0.33, Mean = 5.7, Std Dev = 1.5) (Fig. 3.2a).

The NHMxCALG F_2 population exhibited an approximately normal distribution for FD (Shapiro-Wilk *P* = 0.191, Mean = 191.29, Std Dev = 35.25, NHM = 152.2, KBS = 241.5, F_1 = 192.8), a positively skewed distribution for RTH (Shapiro-Wilk *P* = < 0.001, Mean = 12.25, Std Dev = 4.23, NHM = 8.3, CALG = 22.8, F_1 = 11.9), and an approximately normal distribution for

RRP (Shapiro-Wilk *P* = 0.075, Mean = 6.4, Std Dev = 1.7, NHM = 5.4, CALG = 9.4, F_1 = 6.2) (Fig. 3.2e, f, and g).

SSxSB exhibited an approximately normal distribution for FD (Shapiro-Wilk *P* = 0.96, Mean = 258.40, Std Dev = 37.06, SS = 237.8, SB = 235.2), a positively skewed distribution for RTH (Shapiro-Wilk *P* = 0.0017, Mean = 15.70, Std Dev = 4.23, SS = 17.0, SB = 15.7), and a positively skewed distribution for RRP (Shapiro-Wilk *P* = 0.005, Mean = 6.1, Std Dev = 1.2, SS = 7.1, SB = 6.7) (Fig. 3.2h, i and j). It is of note that for all three of these traits, the parental phenotypes were very similar to each other even though the F_2 population showed similar variation to the other populations.

FD and RTH were significantly correlated in all populations (KxN2010, KxN2016, NHMxCALG, and SSxSB), as were RRP and RTH (Table 3.2). RRP and FD were only significantly correlated in KxN2016.

QTL Mapping

A LOD threshold of 3.0 was determined by the permutation test. FD and RTH were re-mapped in KxN2010 because KASP markers (ClRTH5.1-1 and ClRTH5.1-2) were added to the original map used by Sandlin et al. (2012). In both KxN2010 and KxN2016 QTL for FD were mapped on chromosomes 2 (PVE = 49.5 - 60) and 3 (PVE = 8.1 – 8.4) at the locations of *QFD2.2* and *QFSI3.1,* in accordance with results from Sandlin et al. (2012) (Table 3.3). RTH was mapped on chromosomes 2 (PVE = 51.9 – 52.5) and 5 (PVE = 7.9 – 9.0) for both KxN2010 and KxN2016 (Table 3.3; Fig. 3.3a and b). The QTL locations co-localized with *QFD2.2* and *QRTH5.1* from Sandlin et al. (2012). An additional QTL (*QRTH8.1*) was identified (Table 3.3; Fig. 3.3b) in KxN2016, but not in KxN2010 (Table 3.3; Fig. 3.4a).

QTL mapping for RRP in KxN2010 and KxN2016 revealed three QTL peaks, one each on chromosomes two (PVE = 21.15 – 25.7), three (PVE = 7.0 - 11.37) and five (PVE = 8.27 – 9.9) (Table 3.3; Fig. 3.4c and d). These peaks colocalized with *QFD2.2*, *QFSI3.1* and *QRTH5.1*, respectively.

Marker-Trait Associations

ClFD2.2-1, linked to *QFD2.2*, was significantly associated with FD in KxN2010 (*P* = <0.0001; R^2 = 0.47; KBS/KBS = 182.26; NHM/NHM = 134.57) and KxN2016 (*P* = <0.0001; R^2 = 0.57; KBS/KBS = 180.1; NHM/NHM = 134.8) (Fig. 3.4a and b). ClFD2.2-1 was also significantly associated with RTH and RRP in KxN2010 [RTH (*P* = <0.0001; R^2 = 0.53; KBS/KBS = 11.6; NHM/NHM = 4.63); RRP (*P* = <0.0001; R^2 = 0.26; KBS/KBS = 6.3; NHM/NHM = 4.7)] and KxN2016 [RTH (*P* = <0.0001; R^2 = 0.59; KBS/KBS = 11.45; NHM/NHM = 6.30); RRP (*P* = <0.0001; R^2 = 0.31; KBS/KBS = 6.3; NHM/NHM = 4.7)] (Fig. 3.4c, d, e, and f).

In the KxN RIL population there were a small number of individuals which were heterozygous for the ClSUN-2 (n = 10) or ClRTH5.1-2 (n = 8) loci. ClSUN-2, a functional marker for *QFSI3.1*, was significantly associated with FD [KxN2010 (*P* = 0.0038; R^2 = 0.07; KBS/KBS = 155.2; WT/WT = 174.1); KxN2016 (*P* = 0.005; R^2 = 0.08; KBS/KBS = 155.7; WT/WT = 172.5)] and RRP [KxN2010 (*P* = 0.0026; R^2 = 0.09 KBS/KBS = 6.4; WT/WT = 5.4); KxN2016 (*P* = 0.0087; R^2 = 0.08; KBS/KBS = 6.3; WT/WT = 5.5)] (Figure 3.4g, h, k, and l). ClSUN-2 was not significantly associated with RTH in either year (Fig. 3.4i and j).

ClRTH5.1-2, linked to *QRTH5.1*, was not significantly associated with FD in either KxN2010 or KxN2016 (Fig. 3.4m and n). ClRTH5.1-2 was significantly associated with RTH in KxN2010 (*P* = 0.026; R^2 = 0.05 KBS/KBS = 8.17; NHM/NHM = 10.11), but not in KxN2016 (*P* = 0.055; Fig. 3.4o and p). ClRTH5.1-2 was significantly associated with RRP in KxN2016 (*P* =

0.015; R^2 = 0.06; KBS/KBS = 5.47; NHM/NHM = 6.1), but not KxN2010 (*P* = 0.065; Fig. 3.4q and r). ClRTH5.1-1, the other flanking marker for QRTH5.1, was not significantly associated with RTH or RRP in either KxN2010 or KxN2016, and so was excluded from further analysis.

In both KxN2010 and KxN2016, ClRTH5.1-2 was found to only be significantly associated with RTH in individuals homozygous for the KBS allele at ClFD2.2-1 (Fig. 3.5a and b). In KxN2016, ClRTH5.1-2 was found to only be significantly associated with RRP in individuals homozygous for the KBS allele at ClFD2.2-1 (Fig. 3.5c and d). ClSUN-2 was found to only be significantly associated with RRP in individuals homozygous for the NHM allele at ClFD2.2-1 in KxN2010 and KxN2016 (Fig. 3.5g and h). No interaction was observed between ClSUN-2 and ClFD2.2-1 for RTH (Fig. 3.5 e and f). Heterozygous genotypes were not included in the interaction analyses since there were only a very small number in this RIL population.

In the NHMxCALG population, ClFD2.2-1 was significantly associated with FD (*P* = <0.0001; R^2 = 0.27; KBS/KBS = 220.94; NHM/NHM = 164.56), RTH (*P* = <0.0001; R^2 = 0.46; KBS/KBS = 17.44; NHM/NHM = 8.52) and RRP (*P* = 0.0003; R^2 = 0.22; KBS/KBS = 7.8; NHM/NHM = 5.3) (Fig. 3.6a, b, and c). ClSUN-1 and ClRTH5.1-2 did not show any significant associations with RTH, FD, or RRP in this population. No significant interactions were observed among any pairs of markers in this population (data not shown).

The SSxSB population was only segregating for the ClFD2.2-1 and ClSUN-1 markers. The only significant association observed was between ClSUN-1 and FD (*P* = 0.0047; R^2 = 0.20; WT/WT = 272.29; DEL/DEL = 226.04) (Fig. 3.7d). No other significant associations were observed among ClFD2.2-1 or ClSUN-1 and RTH, FD, and RRP. No significant interactions were observed between the two markers.

Discussion

Rind thickness is an important trait governing the durability of watermelon fruit (Sadrnia et al. 2009). The need for a thick, shippable rind must be balanced against consumer demand for a rind that comprises a small percentage of the overall fruit (Wehner 2008). A more complete understanding of the genetic basis of RTH will allow breeders to more precisely control the trait in breeding populations to produce more desirable fruit.

Our results from KxN2010, KxN2016, NHMxCALG, and SSxSB all confirm the association of ClFD2.2-1 with FD. This adds to the body of evidence for *QFD2.2* as a significant contributor to FD in watermelon across different genetic backgrounds (Sandlin et al. 2012). The KASP assay ClFD2.2-1 reported here should be a useful marker to select for *QFD2.2* in watermelon populations. ClFD2.2-1 was also found to be associated with RTH and RPP in KxN2010, KxN2016, and NHMxCALG. This confirms the results from Sandlin et al. (2012) and Yang et al. (2021), who also reported QTL for RTH in this location. It remains to be determined whether the effects on FD and RTH are caused by closely linked QTL or a single, pleiotropic QTL. Unfortunately, Yang et al. (2020) did not present mapping data for FD in addition to their data for RTH, as it would be interesting to see whether *QFD2.2* and *QRTH2.1* colocalize in additional populations. The lack of association of ClFD2.2-1 with FD, RTH and RRP in SSxSB suggests that different loci are responsible for the variation in these traits in this population.

ClSUN-2 was significantly associated with RRP in KxN2010 and KxN2016. In the study by Sandlin et al. (2012) no QTL for RTH was localized with *QFSI3.1*, despite a significant correlation between RTH and FL in three different populations. We hypothesized that an association with RTH was masked by the large effect of *QRTH2.1* on RTH. The RRP trait, which normalizes RTH for FD, was specifically created in the present study to address this issue. In

melon, a QTL associated with FSI (*QFSI7.1*) colocalized with a QTL for exocarp thickness (ET), analogous to RTH in watermelon (Zhang et al., 2020). *QFSI7.1* is a putative homologue of the consensus QTL *CmFSI7.4* (Pan et al. 2020; Paris et al. 2008). Interestingly one of the candidate genes for *CmFSI7.4* is *CmSUN13-14b*, another SUN family gene (Pan et al., 2020).

ClSUN-1 and ClSUN-2 (functional markers for *QFSI3.1*) was also found to be significantly associated with FD in KxN2010, KxN2016, and SSxSB. This agrees with previously reported results by Sandlin et al. (2012) and Legendre et al. (2020). In tomato, SUN has been shown to increase length via an increase in the number of cells, rather than increase of cell mass, and was not shown to be associated with increases in weight (Wu et al. 2011). The result of this is a longer and narrower tomato. Similarly, in this study the *ClSUN25-26-27a* alleles associated with increased FL (KBS and DEL) were also associated with a decrease in FD in two different populations. This was observed both when comparing the WT/WT genotype to KBS/KBS in KxN2010 and KxN2016, as well as DEL/DEL in SSxSB (Fig. 3.4g, h, and Fig.3.7d). Interestingly, this association (FD and ClSUN-1) was not observed in NHMxCALG, despite CALG possessing the DEL allele responsible for the most elongate phenotype. In a diverse cultivar panel Legendre et al. (2020) observed lower ovary diameter in WT/WT cultivars than DEL/DEL cultivars. However, this association was not observed for mature fruit diameter in the same cultivar panel confirming that in mature fruit the association is dependent on the genetic background.

ClRTH5.1 was significantly associated with RTH and RRP in KxN2010 and KxN2016, either individually (Fig. 3.4o and r) or interacting with CLFD2.2-1 (Fig. 3.5a, b, and d). *QRTH5.1* is unique in that it is the only QTL in the present study that is not colocalized with a known fruit size QTL (*QFD2.2* and *QFSI3.1*). These results support the results of Sandlin et al. (2012)

suggesting that *QRTH5.1* is not colocalized with fruit size QTL. In melon, a QTL on Chromosome 11 associated with ET also did not colocalize with fruit size QTL (Zhang et al. 2020).

The results of this study provide valuable insight into understanding the genetic mechanisms controlling RTH and their relation to other fruit size traits and reveal future avenues of potential investigation. We are currently fine mapping *QFD2.2* to determine whether the association of this locus with FD and RTH is due to pleiotropy or linkage. The ClFD2.2-1 and ClRTH5.1-2 marker assays should prove useful for selection for *QFD2.2* and *QRTH5.1* in watermelon breeding efforts.

References

Breakiron, P.L. 1954. Studies of watermelon loading for rail shipment, 1953. U.S. Department of Agriculture, Agricultural Marketing Service.

Cheng, Y., F. Luan, X. Wang, P. Gao, Z. Zhu, S. Liu, A.M. Baloch and Y. Zhang. 2016. Construction of a genetic linkage map of watermelon (*Citrullus lanatus*) using CAPS and SSR markers and QTL analysis for fruit quality traits. Sci. Hortic. 202:25–31.

Dou, J., S. Zhao, X. Lu, N. He, L. Zhang, A. Ali, H. Kuang and W. Liu. 2018. Genetic mapping reveals a candidate gene (*ClFS1*) for fruit shape in watermelon (*Citrullus lanatus* L.). Theor. Appl. Genet. 131:947–958.

Fall, L.A., J. Clevenger and C. McGregor. 2018. Assay development and marker validation for marker assisted selection of *Fusarium oxysporum* f. sp. *niveum* race 1 in watermelon. Mol. Breed. 38:130.

FAOSTAT. 2020. FAOSTAT Crop Production Data [WWW Document]. URL http://www.fao.org/faostat/en/

Gimode, W., J. Clevenger and C. McGregor. 2019. Fine-mapping of a major quantitative trait locus *Qdff3-1* controlling flowering time in watermelon. Mol. Breed. 40:3.

Kim, K.-H., J.-H. Hwang, D.-Y. Han, M. Park, S. Kim, D. Choi, Y. Kim, G.P. Lee, S.-T. Kim and Y.-H. Park. 2015. Major quantitative trait loci and putative candidate genes for powdery mildew resistance and fruit-related traits revealed by an intraspecific genetic map for watermelon (*Citrullus lanatus var. lanatus*). PLOS ONE 10.

Legendre, R., J. Kuzy and C. McGregor. 2020. Markers for selection of three alleles of *ClSUN25-26-27a* (*Cla011257*) associated with fruit shape in watermelon. Mol. Breed. 40:19.

Meng, L., H. Li, L. Zhang and J. Wang. 2015. QTL IciMapping: Integrated software for genetic linkage map construction and quantitative trait locus mapping in biparental populations. Crop J., Special Issue: Breeding to Optimize Agriculture in a Changing World 3:269–283.

Pan, Y., Y. Wang, C. McGregor, S. Liu, F. Luan, M. Gao and Y. Weng. 2020. Genetic architecture of fruit size and shape variation in cucurbits: a comparative perspective. Theor. Appl. Genet. 133:1–21.

Paris, M.K., J.E. Zalapa, J.D. McCreight and J.E. Staub. 2008. Genetic dissection of fruit quality components in melon (*Cucumis melo* L.) using a RIL population derived from exotic × elite US Western Shipping germplasm. Mol. Breed. 22:405–419.

Perkins-Veazie, P., J.C. Beaulieu and M. Siddiq. n.d. Watermelon, Cantaloupe and Honeydew, p. 549–568. *In* Tropical and Subtropical Fruits. John Wiley & Sons, Ltd.

Poole, C.F. 1944. Genetics of cultivated cucurbits. J. Hered. 35:122–128.

Porter, D. 1937. Inheritance of certain fruit and seed characters in watermelons. Hilgardia 10:489–509.

R Core Team, Rf. and others. 2013. R: A language and environment for statistical computing. R foundation for statistical computing Vienna, Austria.

Sadrnia, H., A. Rajabipour, A. Jafari, A. Javadi, Y. Mostoufi, T. Bagherpour and N.M. Khojasteh. 2009. Mechanical failure of two varieties of watermelon under quasi static load. Iran. J. Biosyst. Eng. 40:169–174.

Sandlin, K., J. Prothro, A. Heesacker, N. Khalilian, R. Okashah, W. Xiang, E. Bachlava, D.G. Caldwell, C.A. Taylor, D.K. Seymour, V. White, E. Chan, G. Tolla, C. White, D. Safran, E. Graham, S. Knapp and C. McGregor. 2012. Comparative mapping in watermelon [*Citrullus lanatus* (Thunb.) Matsum. et Nakai]. Theor. Appl. Genet. 125:1603–1618.

Schindelin, J., I. Arganda-Carreras, E. Frise, V. Kaynig, M. Longair, T. Pietzsch, S. Preibisch, C. Rueden, S. Saalfeld, B. Schmid, J.-Y. Tinevez, D.J. White, V. Hartenstein, K. Eliceiri, P. Tomancak and A. Cardona. 2012. Fiji: an open-source platform for biological-image analysis. Nat. Methods 9:676–682.

Tanaka, Y. 1957. Report of the international committee on genetic symbols and nomenclature. Int. Union Biol. Sci. B 30:1–6.

Untergasser, A., H. Nijveen, X. Rao, T. Bisseling, R. Geurts and J.A.M. Leunissen. 2007. Primer3Plus, an enhanced web interface to Primer3. Nucleic Acids Res. 35:W71–W74.

Van Ooijen, J. 2006. JoinMap 4: Software for the calculation of genetic linkage maps in experimental populations. Kyazma BV, Wageningen, Netherlands.

Weetman, L. 1937. Inheritance and correlation of shape, size and color in the watermelon, Citrullus Vulgaris Schrad. Iowa Agric. Home Econ. Exp. Stn. Res. Bull. 20.

Wehner, T.C. 2008. Watermelon, p. 381–418. *In* J. Prohens & F. Nuez (eds.). Vegetables I: Asteraceae, Brassicaceae, Chenopodicaceae, and Cucurbitaceae, Handbook of Plant Breeding. Springer New York, New York, NY.

Wehner, T.C. 2012. 2012 Gene List for Watermelon [WWW Document]. Cucurbit Genet. Coop. URL https://cucurbit.info/2012/07/2012-gene-list-for-watermelon/

Wickham, H. 2016. ggplot2: elegant graphics for data analysis. Springer-Verlag New York.

Wu, S., H. Xiao, A. Cabrera, T. Meulia and E. van der Knaap. 2011. *SUN* regulates vegetative and reproductive organ shape by changing cell division patterns. Plant Physiol. 157:1175–1186.

Yang, T., S. Amanullah, J. Pan, G. Chen, S. Liu, S. Ma, J. Wang, P. Gao and X. Wang. 2021. Identification of putative genetic regions for watermelon rind hardness and related traits by BSA-seq and QTL mapping. Euphytica 217:19.

Zhang, T., Z. Ding, J. Liu, B. Qiu and P. Gao. 2020. QTL mapping of pericarp and fruit-related traits in melon (Cucumis melo L.) using SNP-derived CAPS markers. Sci. Hortic. 265:109243.

Table 3.1: KASP assays ClRTH-5.1-1, ClRTH-5.1-2, and ClFD2.2-1. ClRTH-5.1-1 and ClRTH-5.1-2 are flanking markers for *QRTH5.1*, while ClFD2.2-1 is linked to *QFD2.2* in the KxN population.

KASP Assay	Ta (°C)	Target	Primer type	Primer sequence (5′-3′)	Allele
ClRTH-5.1-1	57	SNP: UGA5_27816929	FAM	GAAGGTGACCAAGTTCATGCTAGTTCAACACGTAC TAATCCCACTTGC	NHM
			VIC	GAAGGTCGGAGTCAACGGATTAGTTCAACACGTAC TAATCCCACTTGG	KBS
			Reverse	CACAAGGGTTAGACAGAGGGTAAAGATAT	
ClRTH-5.1-2	57	SNP: UGA5_28507930	FAM	GAAGGTGACCAAGTTCATGCTAAGGAGGCTTGAGT TTTGTTAATCTAGACT	NHM
			VIC	GAAGGTCGGAGTCAACGGATTGGAGGCTTGAGTTT TGTTAATCTAGACC	KBS
			Reverse	TACAAAGGCTCTCTAGATCATCACACTTA	
ClFD2.2-1	54.8	SNP: NW0249226	FAM	GAAGGTGACCAAGTTCATGCTAGTGGAGTTCTTTTC TGATTATGGA	KBS
			VIC	GAAGGTCGGAGTCAACGGTTAGTGGAGTTCTTTTCT GATTATGGC	NHM
			Reverse	GCGGGTGTCAATTGCGGAAC	

`

Table 3.2: Pearson correlations for FD, RTH, and RRP in the (a) KxN2010, (b) KxN2016, (c) NHMxCALG, and (d) SSxSB populations. Asterisks indicate significant correlations ($P < 0.05$).

(a) KxN2010		FD	RTH
	RTH	0.71*	
	RRP	0.09	0.45*
(b) KxN2016		FD	RTH
	RTH	0.71*	
	RRP	0.30*	0.87*
(c) NHMxCALG		FD	RTH
	RTH	0.62*	
	RRP	0.07	0.81*
(d) SSxSB		FD	RTH
	RTH	0.47*	
	RRP	-0.20	0.74*

Table 3.3: QTL mapping results for FD, RTH, and RRP mapped in KxN2010 and KxN2016. KxN2010 was re-mapped using raw data from Sandlin et al. (2012) after the addition of ClRTH5.1-1 and ClRTH5.1-2 in the genetic map.

Trait	QTL	Chr.	Max LOD	PVE	Max LOD Position	1-LOD CI Left	1-LOD CI Right
				2010			
FD	*QFD2.2*	2	22.7	49.5	78.0	76.5	80.5
FD	*QFSI3.1*	3	5.4	8.1	79.0	77.5	79.5
RTH	*QFD2.2*	2	25.7	51.9	77.0	75.5	78.5
RTH	*QRTH5.1*	5	5.6	7.9	212.0	208.5	214.5
RRP	*QFD2.2*	2	10.6	21.2	75.0	72.5	78.5
RRP	*QFSI3.1*	3	5.3	11.4	72.0	64.5	77.5
RRP	*QRTH5.1*	5	3.9	8.3	217.0	212.5	225.5
				2016			
FD	*QFD2.2*	2	30.4	60.0	78.0	76.5	80.5
FD	*QFSI3.1*	3	6.3	8.4.0	73.0	67.5	79.5
RTH	*QFD2.2*	2	30.6	52.5	76.0	74.5	77.5
RTH	*QRTH5.1*	5	7.7	9.0	213.0	211.5	214.5
RTH	*QRTH8.1*	8	3.2	3.7	6.0	0	7.5
RRP	*QFD2.2*	2	13.3	25.7	76.0	73.5	77.5
RRP	*QFSI3.1*	3	3.5	7.0	71.0	59.5	77.5
RRP	*QRTH5.1*	5	5.7	9.9	213.0	210.5	214.5

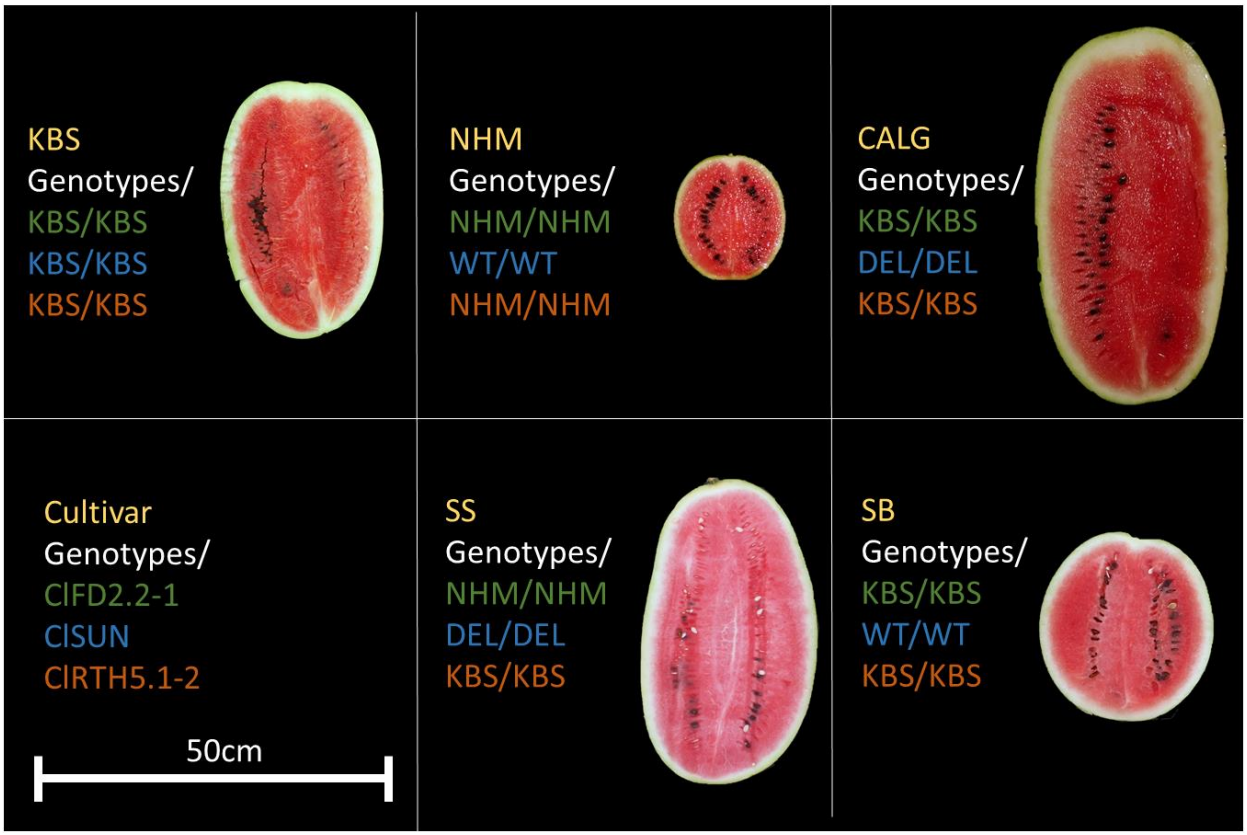

Figure 3.1: Phenotypes and genotypes for ClFD2.2-1, ClSUN-1 and ClSUN-2, and ClRTH5.1-2 for the parents of the populations used in this study. Parents were grown in 2018 and photographed by Legendre *et al*. (2020).

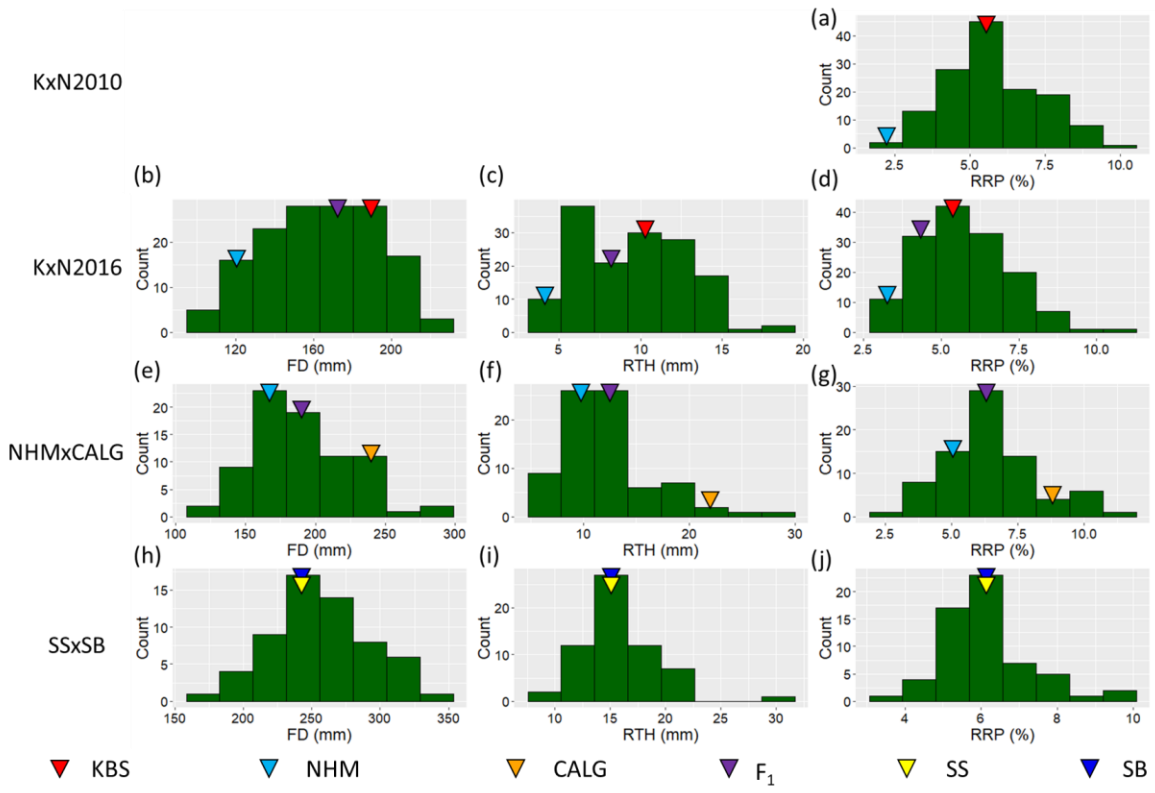

Figure 3.2: Histograms of the phenotypic data showing RRP for KxN2010 and FD. RTH, and RRP for KxN2016, NHMxCALG, and SSxSB. The phenotypic values of the parents and F_1 of the populations are indicated by the following colors of triangle: KBS (red), NHM (blue), CALG (orange), SS (yellow), and SB (blue) and F_1 (purple).

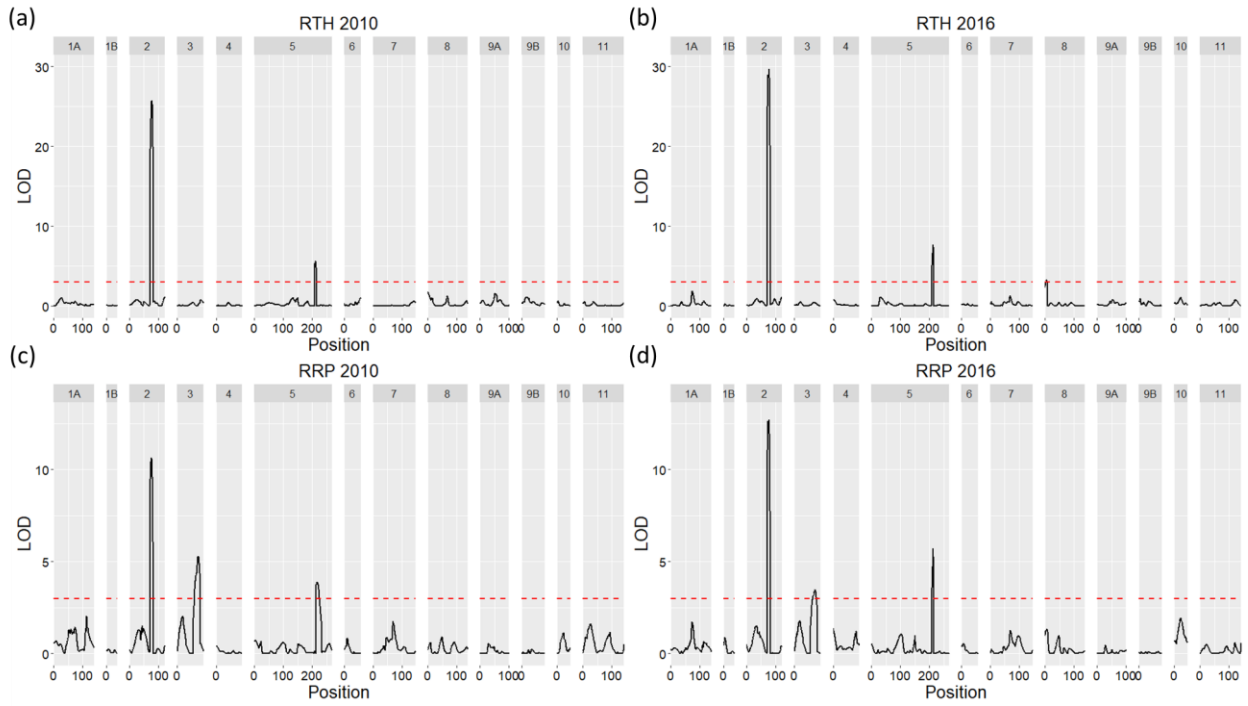

Figure 3.3: QTL mapping of RTH (a and b) and RRP (c and d) in KxN2010 and KxN2016. The red line represents the LOD threshold.

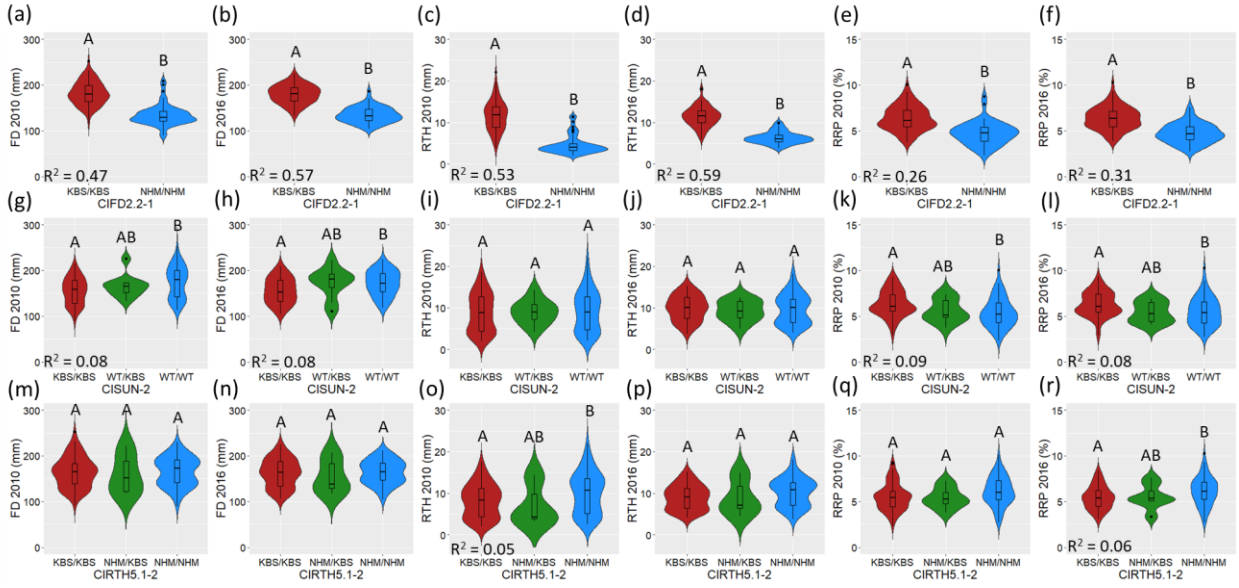

Figure 3.4: Marker-phenotype associations of ClFD2.2-1, ClSUN-2, and ClRTH5.1-2 with FD (a, b, g, h, m, and n), RTH (c, d, i, j, o, and p), and RRP (e, f, k, l, q, and r) for KxN2010 and KxN2016 (n = 147). Different letters above plots indicate significant statistical differences.

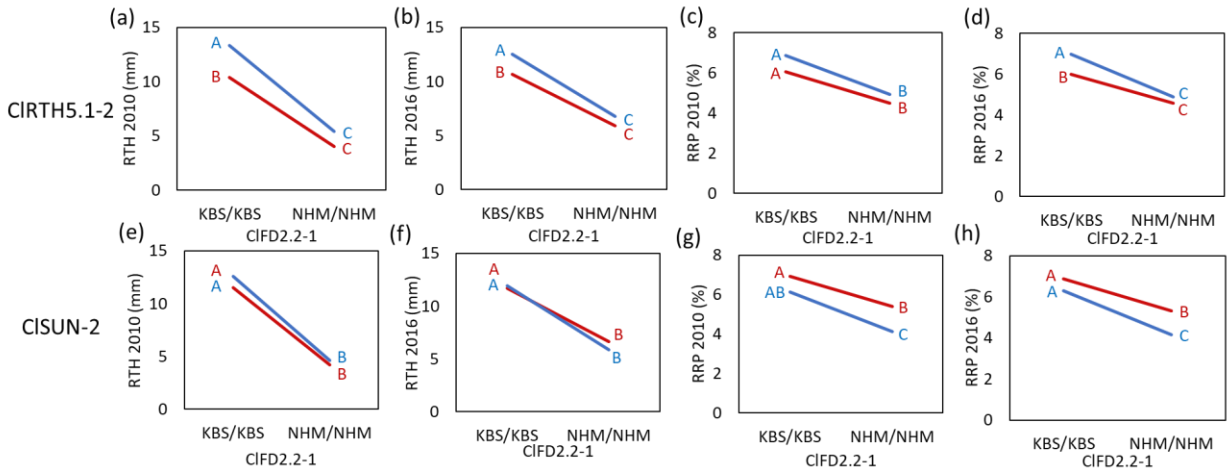

Figure 3.5: The interaction between the effects of ClFD2.2-1(x-axis) with ClRTH5.1-2 (a, b, c, and d) and ClSUN-2 (e, f, g, and h) on RTH and RRP in KxN2010 and KxN2016. For the ClRTH5.1-2 graphs, the KBS/KBS individuals are represented by the red line while the NHM/NHM individuals are represented by the blue line. For the ClSUN-2 graphs the KBS/KBS individuals are represented by the red line while the WT/WT (NHM/NHM) individuals are represented by the blue line. Different letters above plots indicate statistically significant differences.

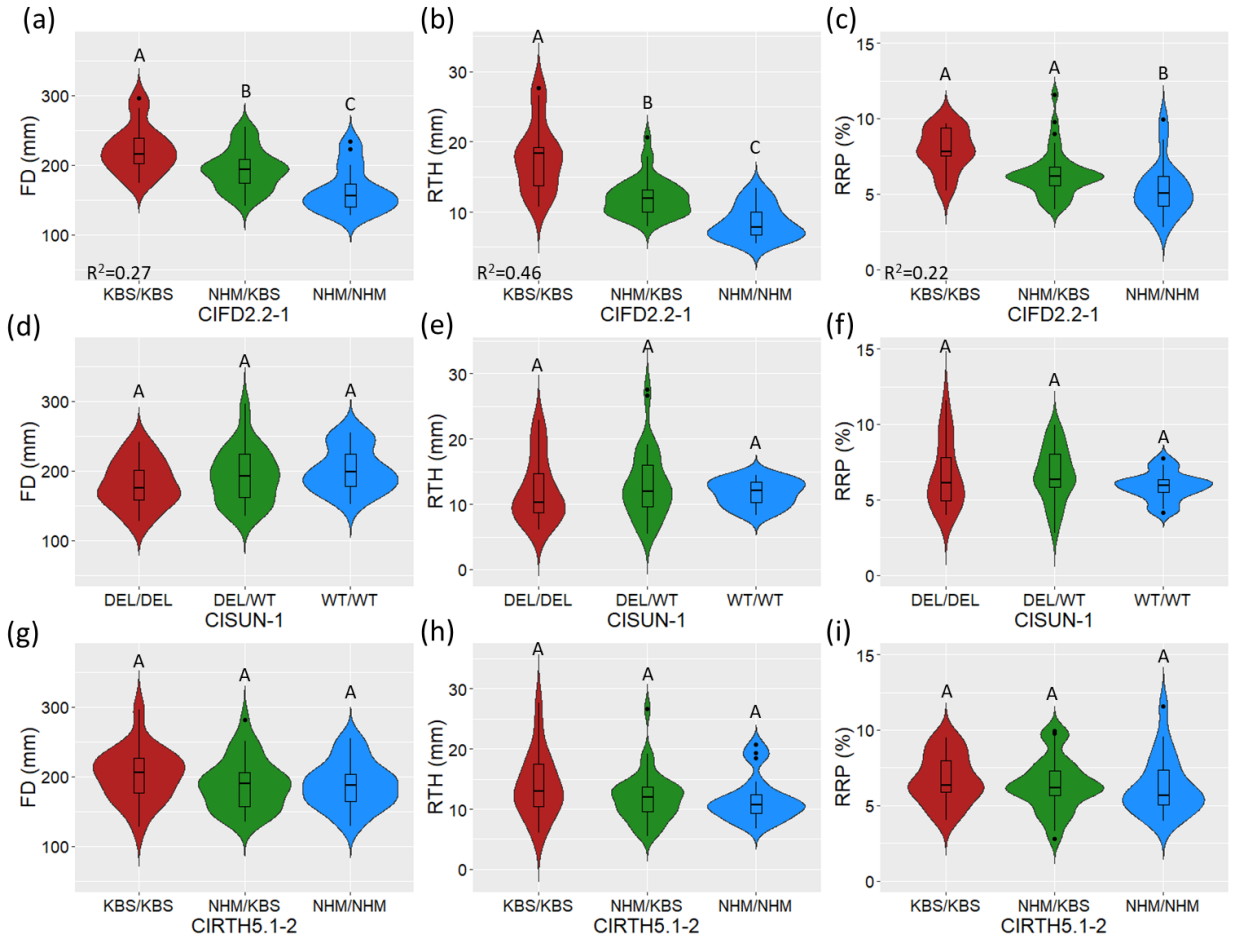

Figure 3.6: Marker-phenotype associations of ClFD2.2-1, ClSUN-1, and ClRTH5.1-2 with FD (a, d, and g), RTH (b, e, and h), and RRP (c, f, and i) in the NHMxCALG F_2 population (n = 86). Different letters above plots indicate statistically significant differences.

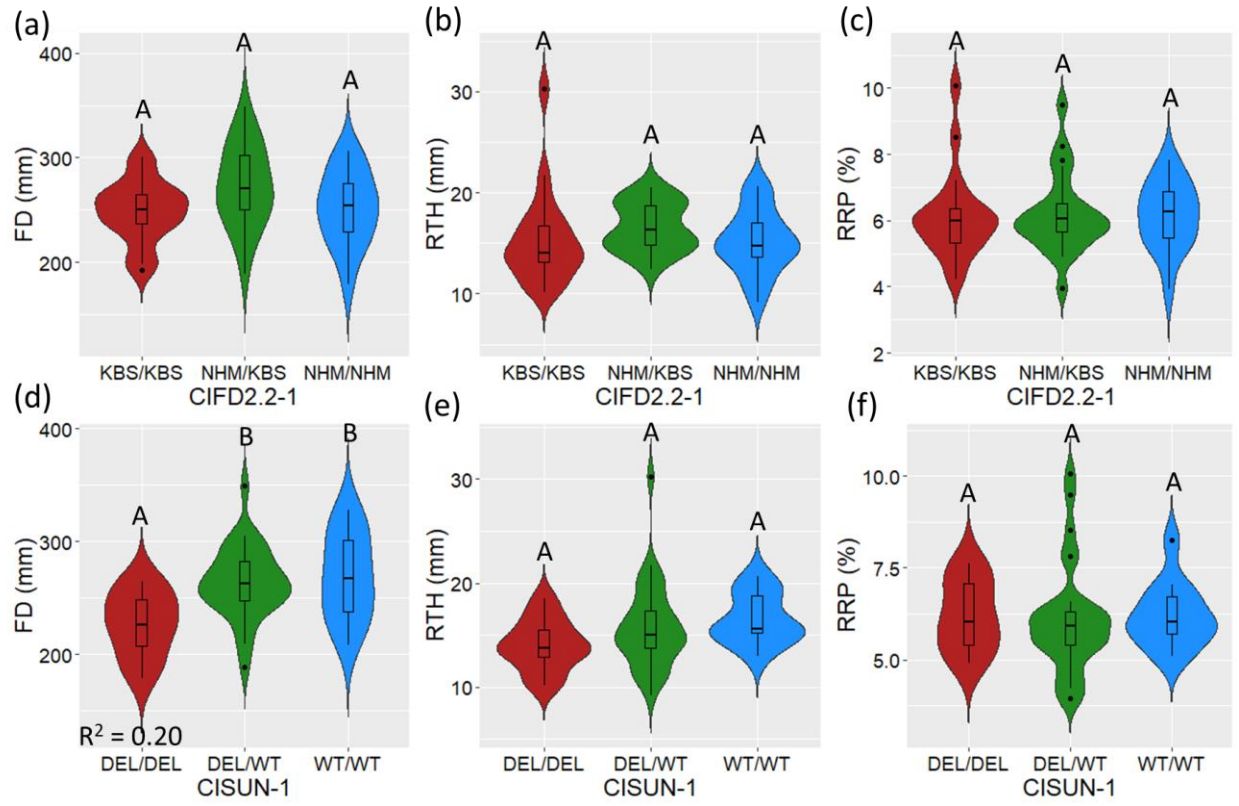

Figure 3.7: Marker-phenotype association of ClFD2.2-1 and ClSUN-1 with FD (a and d), RTH (b and e), and RRP (c and f) in the SSxSB F_2 population (n = 66). Different letters above each plot indicate statistically significant differences.

CHAPTER 4

CONCLUSIONS

Watermelon is a globally important horticultural crop with a worldwide annual planting of over 3 million hectares (FAOSTAT 2020). The United States is one of the top producers globally, with Georgia alone accounting for over $180 million worth of production on approximately 8,900 hectares in 2019 (2019 Farm Gate Value Report 2020). While that may seem like an impressive value, there are many factors that cause economic losses for farmers, driving production numbers down. Of those factors, one of the most important is losses to disease pressure (Little 2020). Cracking or splitting of fruit during shipping is another issue that can lead to economic losses for the watermelon industry (Breakiron 1954). This study examined two traits, gummy stem blight (GSB) resistance and rind thickness (RTH), which help limit the severity of those losses.

Gummy stem blight is one of the main fungal disease pressures facing watermelon in Georgia. It is responsible for a significant portion of the over 33.3 million dollars in disease losses and control costs faced by Georgia farmers every year (Little 2020). GSB is caused by three distinct species of *Stagonosporopsis* fungi, *S. citrulli, S. cucurbitacearum,* and *S. caricae* (Stewart et al. 2015).

A resistant accession of citron melon (PI 189225, *C. amarus)* was used as a parent in a cross with Sugar Baby (*C. lanatus*) to develop an F_2 population. Seed from this population was phenotyped for resistance to *S. citrulli* isolate 12178A. Four QTL for resistance to *S. citrulli* were identified using QTLSeq (Takagi et al. 2013). *Qgsb5.2* was confirmed using QTL mapping of the region of interest. *Qgsb5.2* represents a distinct QTL from those identified previously (Ren et al.

2019, Gimode et al. 2021, Lee et al. 2021). Two other the studies used the same resistance germplasm (PI 189225) as the current study, but different isolates of GSB-causing fungi (Ren et al. 2019; Lee et al. 2021). This, combined with the low PVE values of all these QTL demonstrates that breeders will likely require a pyramid of QTL in order to obtain an effective resistance level in the field. Gimode et al. (2021) used the same isolate as the current study, but a different resistant PI. Combining those QTL with *Qgsb5.1* would likely allow breeders to develop a watermelon with a previously unmatched level of resistance to *S. citrtulli,* the species of GSB causing *Stagonosporopsis* most commonly found in Georgia and other southeastern states (Li et al. 2016).

In addition to being protected from disease, it is also important for watermelon fruit to be protected from damage during shipping. Rind thickness is an important factor in determining the durability of watermelon fruit, with a thick rind improving the suitability of the fruit for packing and shipping. This desire for thick rind must be balanced against consumer preferences for a relatively thin rind (Wehner 2008). A better understanding of the mechanisms controlling rind thickness would be beneficial to breeders as they strive to meet these conflicting demands.

In order to elucidate these issues, this study re-examined two QTL contributing to RTH which were identified by Sandlin et al. (2012) in the Klondike Black Seeded × New Hampshire Midget (KxN2010) recombinant inbred line population. A second year of data was collected for the KxN population (KxN2016), as well as from two genetically distinct F_2 populations [New Hampshire Midget × Calhoun Gray (NHMxCALG), and Sun Sugar × Sugar Baby (SSxSB)]. This study also examined a new trait, "Rind Ratio Percentage" (RRP), which is calculated by the following formula: $\frac{RTH}{FD}\ x\ 100$. QTL mapping of KxN2016 identified QTL for RTH as well as fruit diameter (FD) (*QFD2.2,* & *QRTH5.1*) which colocalized with those from the KxN2010 QTL mapping. QTL mapping also identified QTL for RRP which colocalized with the location of

Cla011257, the gene responsible for *QFSI3.1* and a homolog of the SUN gene, which controls fruit shape by increasing cell division along the proximal-distal axis of the fruit (Kim et al. 2015).

Marker trait associations for markers (ClFD2.2-1, ClSUN-1, ClRTH5.1-2) associated with these regions were examined in three populations (KxN2010, KxN2016, NHMxCALG, and SSxSB). Data from KxN2010 and KxN2016 showed significant associations between RTH and *QFD2.2* and *QRTH5*. *QRTH5.1* was shown to only have a significant effect for individuals with the KBS/KBS genotype at *QFD2.2* as evidenced by marker-marker interactions. RRP was also significantly associated with *QFD2.2*, *QFSI3.1,* and *QRTH5.1* in KxN2016. These same marker associations were examined in the NHMxCALG and SSxSB populations. Results from NHMxCALG show that there was a significant association between ClFD2.2-1 and RTH, FD, and RRP. These associations with ClFD2.2-1 were not observed in SSxSB. While this study has conclusively shown the effects of *QFD2.2, QRTH5.1,* and *QFSI3.1* on RTH and RRP in the KxN genetic background, it remains unclear if these QTL will have a significant association with these traits in a large portion of the watermelon germplasm used by breeders.

These studies identified QTL and/or developed marker assays for QTL for GSB resistance, (*Qgsb5.2*), FD (*QFD2.2*) and RTH (*QRTH5.1*) and expands the toolbox available to watermelon breeders in designing more disease resistant and durable watermelon.

References

2019 Farm Gate Value Report. 2020. University of Georgia Center for Agribusiness and Economic Development.

Breakiron, P.L. 1954. Studies of watermelon loading for rail shipment, 1953. U.S. Department of Agriculture, Agricultural Marketing Service.

FAOSTAT. 2020. FAOSTAT Crop Production Data. 1 July 2021. <http://www.fao.org/faostat/en/>

Gimode, W., K. Bao, Z. Fei and C. McGregor. 2021. QTL associated with gummy stem blight resistance in watermelon. Theor. Appl. Genet. 134:573–584.

Kim, K.-H., J.-H. Hwang, D.-Y. Han, M. Park, S. Kim, D. Choi, Y. Kim, G.P. Lee, S.-T. Kim and Y.-H. Park. 2015. Major quantitative trait loci and putative candidate genes for powdery mildew resistance and fruit-related traits revealed by an intraspecific genetic map for watermelon (*Citrullus lanatus var. lanatus*). PLOS ONE 10.

Lee, E.S., D.-S. Kim, S.G. Kim, Y.-C. Huh, C.-G. Back, Y.-R. Lee, M.I. Siddique, K. Han, H.-E. Lee and J. Lee. 2021. QTL mapping for gummy stem blight resistance in watermelon (*Citrullus spp.*). Plants 10:500.

Little, E. 2020. 2019 Georgia plant disease loss estimates. University of Georgia Cooperative Extension.

Pan, Y., Y. Wang, C. McGregor, S. Liu, F. Luan, M. Gao and Y. Weng. 2020. Genetic architecture of fruit size and shape variation in cucurbits: a comparative perspective. Theor. Appl. Genet. 133:1–21.

Ren, R., J. Xu, M. Zhang, G. Liu, X. Yao, L. Zhu and Q. Hou. 2019. Identification and molecular mapping of a gummy stem blight resistance gene in wild watermelon (*Citrullus amarus*) germplasm PI 189225. Plant Disease 104:16–24.

Li, H.-X. and M.T. Brewer. 2016. Spatial genetic structure and population dynamics of gummy stem blight fungi within and among watermelon fields in the southeastern United States. Phytopathology 106:900–908.

Takagi, H., A. Abe, K. Yoshida, S. Kosugi, S. Natsume, C. Mitsuoka, A. Uemura, H. Utsushi, M. Tamiru, S. Takuno, H. Innan, L.M. Cano, S. Kamoun and R. Terauchi. 2013. Qtl-seq: rapid mapping of quantitative trait loci in rice by whole genome resequencing of DNA from two bulked populations. The Plant Journal 74:174–183.

Wehner, T.C. 2008. Watermelon, p. 381–418. *In* J. Prohens & F. Nuez (eds.). Vegetables I: Asteraceae, Brassicaceae, Chenopodicaceae, and Cucurbitaceae, Handbook of Plant Breeding. Springer New York, New York, NY.